

1 **RUNNING TITLE:**

2 Novel biogenic plastid signals

3

4 **AUTHOR FOR CORRESPONDENCE:**

5 Thomas Pfannschmidt

6 LPCV, CNRS, CEA, INRA, Université Grenoble-Alpes, BIG, 38000, Grenoble, France

7 E-mail : [Thomas.Pfannschmidt@univ-grenoble-alpes.fr](mailto:Thomas.Pfannschmidt@univ-grenoble-alpes.fr)

8 (Fax: +33 438785196; Tel: +33 )

9

10 **Light and plastid signals regulate different sets of genes in the albino**  
11 **mutant pap7-1**

12 **Authors:** Björn Grübler<sup>1</sup>, Livia Merendino<sup>1</sup>, Sven O. Twardziok<sup>2</sup>, Morgane Mininno<sup>1</sup>,  
13 Guillaume Allore<sup>1</sup>, Fabien Chevalier<sup>1</sup>, Monique Liebers<sup>1</sup>, Robert Blanvillain<sup>1</sup>, Klaus F. X.  
14 Mayer<sup>2</sup>, Silva Lerbs-Mache<sup>1</sup>, Stéphane Ravanel<sup>1</sup>, Thomas Pfannschmidt<sup>1</sup>

15 <sup>1</sup> LPCV, CNRS, CEA, INRA, Université Grenoble-Alpes, BIG, 38000, Grenoble, France ; <sup>2</sup>  
16 Plant Genome and Systems Biology, Helmholtz Zentrum München, 85764 Neuherberg,  
17 Germany

18

19 **AUTHOR CONTRIBUTIONS**

20 B.G., L.M., R.B., S.R., T.P. designed the research and/or experiments; B.G., L.M., M.M.,  
21 G.A., F.C., M.L., R.B. performed research; K.M. contributed new computational tools; B.G.,  
22 L.M., S.T., S.L., S.R., T.P. analyzed data; T.P. wrote the article with the help of all co-  
23 authors.

24

25 **FUNDING INFORMATION**

26 This work was supported by grants from the Deutsche Forschungsgemeinschaft to T.P.  
27 (PF323-5-2) and the DFG research group FOR 804. The study received also institutional

28 financial support from the French National Research Agency (ANR-10-LABEX-04 GRAL  
29 Labex, Grenoble Alliance for Integrated Structural Cell Biology).

30

31 **ONE-SENTENCE SUMMARY**

32 The albino pap7-1 mutant of Arabidopsis reveals the relative impact of light and  
33 plastid developmental stage on the expression of nuclear genes involved in  
34 metabolism and photosynthesis.

35 **ABSTRACT**

36 Plants possessing dysfunctional plastids due to defects in pigment biosynthesis or translation  
37 are known to repress photosynthesis-associated nuclear genes (PhANGs) *via* retrograde  
38 signals from the disturbed organelles towards the nucleus. These signals are thought to be  
39 essential for proper biogenesis and function of the plastid. Mutants lacking plastid-encoded  
40 RNA polymerase-associated proteins (PAPs) display a genetic arrest in eoplast-chloroplast  
41 transition leading to an albino phenotype in the light. Retrograde signaling in these mutants,  
42 thus, could be expected to be similar as under conditions inducing plastid dysfunction. In  
43 order to answer this question we performed plastome- and genome-wide array analyses in  
44 the *pap7-1* mutant of *Arabidopsis*. In parallel, we determined the potential overlap with light-  
45 regulated expression networks. To this end we performed a comparative expression profiling  
46 approach using light- and dark-grown wild-type plants as relative control for the expression  
47 profiles obtained from light-grown *pap7-1* mutants. Our data indicate a specific impact of  
48 retrograde signals on metabolism related genes in *pap7-1* mutants reflecting the starvation  
49 situation of the albino seedlings. In contrast light regulation of PhANGs and other nuclear  
50 gene groups appears to be fully functional in this mutant indicating that a block in chloroplast  
51 biogenesis *per se* does not repress expression of them as suggested by earlier studies. Only  
52 genes for light harvesting complex proteins displayed a significant repression indicating an  
53 exclusive retrograde impact on this gene family. Our results indicate that chloroplasts and  
54 arrested plastids each emit specific signals that control different target gene modules both in  
55 positive and negative manner.

56

57

## 58 INTRODUCTION

59 The build-up of the photosynthetic machinery during photomorphogenesis of angiosperms  
60 requires a tight coordination of nuclear and plastid gene expression as the photosynthesis  
61 genes are distributed over both genetic compartments (Waters and Langdale, 2009; Arsovski  
62 et al., 2012; Pogson et al., 2015). This coordination is achieved by a mutual information  
63 exchange between nucleus and plastids that is called anterograde (from nucleus towards  
64 plastids) and retrograde (from plastids towards nucleus) signaling. This mutual signaling has  
65 been studied extensively, but is still far from being understood (Chi et al., 2013; Chan et al.,  
66 2016; de Souza et al., 2016; Kleine and Leister, 2016). The retrograde plastidial signals that  
67 are identified so far are numerous and of very diverse nature (see below). A recent proposal  
68 categorizes them according to their respective developmental context into i) biogenic signals  
69 that act during early chloroplast biogenesis (e.g. during germination and seedling  
70 development) controlling proper organelle establishment and ii) operational signals that are  
71 sent from well-developed chloroplast in later plant stages in order to mediate acclimation  
72 responses to environmental changes (Pogson et al., 2008). This concept has been expanded  
73 by the proposal of a third category, degradational signals sent from chloroplasts during  
74 senescence and that mediate nutrient allocation when plastids are finally degraded  
75 (Pfannschmidt and Munne-Bosch, 2013).

76 Current models suggest the action of various plastid metabolites, protein factors, reactive  
77 oxygen species (ROS) as well as redox signals from photosynthesis as mediators of  
78 retrograde signaling. The list of identified metabolites and oxidation products includes haem,  
79 singlet oxygen or hydrogen peroxide, carotenoid oxidation products, 3'-phosphoadenosine-  
80 5'-phosphate, methylerythritol cyclodiphosphate and oxo-phytyldienoic acid (OPDA) (Lee et  
81 al., 2007; Galvez-Valdivieso et al., 2009; Estavillo et al., 2011; Woodson et al., 2011; Ramel  
82 et al., 2012; Xiao et al., 2012; Park et al., 2013). Proteins proposed to act as plastid signals  
83 include envelope-tethered eukaryotic transcription factors TFIIB-like and PTM, both being  
84 released from the outer plastid membrane by targeted proteolysis (Lagrange et al., 2003;  
85 Sun et al., 2011) and a plastid localized Whirly1 protein that is released from plastids upon  
86 stress (Isemer et al., 2012). A very recent study, however, puts this particular function of  
87 PTM in retrograde signaling into question (Page et al., 2017). Most of these retrograde  
88 signaling molecules are discussed as stress signals operating from fully developed  
89 chloroplasts. However, their mode of action and their potential interactions are largely not  
90 understood and many questions concerning their function and interaction remain  
91 unanswered.

92 Biogenic signals that are proposed to be active only during proplastid-to-chloroplast  
93 conversion are even less understood and the retrograde signals that contribute to chloroplast

94 biogenesis still remain to be identified. One major difficulty in studying biogenic plastid  
95 signal(s) is the large functional and temporal overlap with the photoreceptor-controlled light  
96 signaling network. Already early studies in this research field revealed that it is difficult to  
97 separate the influences of plastid signals on nuclear gene expression from those initiated by  
98 light as both occur at the same time range and on the same target genes. Transgenic  
99 reporter gene approaches could demonstrate that plastid and light signals do even use the  
100 same promoter elements in front of their target genes (Kusnetsov et al., 1996; Sullivan and  
101 Gray, 2002; Brown et al., 2005). Recent studies suggest a close functional relationship  
102 between both control modes and it has been proposed that plastid signals can even remodel  
103 light signaling pathways from positive into negative signals and *vice versa* (Ruckle et al.,  
104 2007; Ruckle et al., 2012). Another recent study, however, suggests that light and plastid  
105 signaling routes act antagonistically in nuclear gene expression (Martin et al., 2016). Thus,  
106 the determined relative impact of light and retrograde signals on nuclear gene expression  
107 remains unclear.

108 Coordination of nuclear and plastid gene expression is also important for the establishment  
109 of the gene expression machinery in plastids and, in particular, for plastid localized RNA  
110 polymerases. A nuclear-encoded single-subunit phage-type RNA polymerase (NEP) and a  
111 plastid-encoded prokaryotic-type RNA polymerase (PEP) exist in plastids of green vascular  
112 plants. PEP is composed of four plastid-encoded subunits and 12 nuclear-encoded  
113 polymerase-associated proteins (PAPs). Furthermore, in *Arabidopsis* PEP requires  
114 interaction with six nucleus-coded sigma factors for promoter recognition (Lerbs-Mache,  
115 2011; Borner et al., 2015; Pfannschmidt et al., 2015).

116 These RNA polymerases are key players in the coordination of the gene expression between  
117 plastids and the nucleus as they transcribe the genetic information within the plastids in a  
118 developmentally well-coordinated manner that is especially important during the early stages  
119 of seedling development (Liebers et al., 2017). Although not all details are known yet it is  
120 largely accepted that NEP represents the dominant plastid RNA polymerase activity in  
121 plastids of non-green embryonic and meristematic cells. Its activity is essential for the  
122 expression of the plastid *rpo* genes and for the establishment of the core enzyme of PEP  
123 (Liere et al., 2011). During the course of chloroplast biogenesis this basal PEP core enzyme  
124 becomes then decorated with PAPs. As far as known PAPs are induced in their expression  
125 by light and *in silico* analyses strongly suggest that they represent a tight regulon (Steiner et  
126 al., 2011; Pfannschmidt et al., 2015). The precise structural and functional roles of PAPs  
127 within the PEP complex and their regulatory relationship to plastid (and potentially nuclear)  
128 transcription are largely unknown and subject to current research.

129 Interestingly, all PAPs cause the same phenotypic consequences when their corresponding  
130 genes are inactivated. In *Arabidopsis* but also in maize or rice inactivation of *pap* genes  
131 result in albino, ivory or pale-green phenotypes with arrested plastid development. Plastids of  
132 such mutants do not develop a thylakoid membrane system and display enhanced transcript  
133 accumulation of NEP-dependent genes while transcript accumulation of PEP-dependent  
134 genes (including those for photosynthesis) is typically diminished (Pfalz and Pfannschmidt,  
135 2013). This expression profile of plastid-encoded genes is reminiscent of those found in  
136 plastid *rpo* deletion mutants of tobacco (Hajdukiewicz et al., 1997; De Santis-Maclossek et  
137 al., 1999; Legen et al., 2002). The best possible explanation for this effect to date is that the  
138 lack of any of the PAPs either prevents the formation or compromises the stability of the PEP  
139 complex in developing chloroplasts. This, subsequently, leads to a lack of PEP-dependent  
140 processes and a concomitant arrest in chloroplast biogenesis since PEP is responsible for  
141 the expression of photosynthesis and tRNA genes (Williams-Carrier et al., 2014). It is  
142 important to note that the PAP assembly around the PEP core does not occur in the dark  
143 (Pfannschmidt and Link, 1994) and, consequently, *pap* mutants perform a normal  
144 skotomorphogenesis remaining undistinguishable from wildtype (Gilkerson et al., 2012).  
145 Expression and assembly of PAPs around the PEP core complex, thus, appear to represent  
146 a key initiation step in the formation of chloroplasts. The corresponding mutants represent,  
147 therefore, a useful tool to study the impact of a blocked transition from proplastids (or  
148 eoplasts) towards chloroplasts on the photomorphogenic program during seedling  
149 development.

150 Here, we present a study using the *Arabidopsis pap7-1* mutant in order to elucidate the  
151 relative impact of arrested plastid development and light on nuclear gene expression. Like  
152 other PAPs the PAP7/pTAC14 protein has been identified as a subunit of the plastid  
153 encoded RNA polymerase (PEP) (Pfalz et al., 2006; Steiner et al., 2011). In *Arabidopsis* the  
154 corresponding gene (At4g20130) codes for a protein of 55 kDa that contains a chloroplast  
155 transit peptide, a predicted SET domain characteristic of protein lysine methyltransferases  
156 and a putative Rubisco LSMT substrate-binding domain. The precise function of the protein  
157 within the PEP complex as well as any evidence for methylation activity is still elusive, but an  
158 inactivation of the *pap7-1/ptac14* gene in *Arabidopsis* results in an albino phenotype that is  
159 viable only on sucrose-supplemented medium (Gao et al., 2011; Steiner et al., 2011). The  
160 mutant displays all the molecular and structural features described for other *pap* mutants  
161 (Gao et al., 2011) that we proposed to name as the PAP syndrome. Our study provides a  
162 detailed catalogue of target gene modules at plastome and genome-wide levels and gives  
163 unexpected novel clues into the involvement of biogenic retrograde signaling in the  
164 regulation of nuclear genes for photosynthesis and metabolism.



## 166 RESULTS

### 167 ***Arabidopsis pap7-1* mutants exhibit normal photomorphogenic development but never** 168 **develop chloroplasts**

169 Homozygous *pap7-1* mutant seedlings are known to develop an albino phenotype when  
170 grown in the light (Gao et al., 2011; Steiner et al., 2011). However, when grown in the dark  
171 homozygous mutants develop a fully normal etiolated phenotype that remains  
172 macroscopically undistinguishable from heterozygous mutant or WT seedlings. They can be  
173 identified only by the missing greening process upon subsequent illumination (Fig. 1A), while  
174 they otherwise demonstrate a WT-like morphology. Grown directly in light without preceding  
175 dark phase homozygous mutants show light-induced repression of hypocotyl elongation,  
176 opening of the apical hook and separation and expansion of the cotyledons (Fig. 1B). When  
177 kept on standard growth medium without additional carbon source *pap7-1* mutant seedlings  
178 could not develop further than the cotyledon stage, started to bleach, became transparent  
179 and finally died (Fig. 1B). On sucrose supplemented medium, however, *pap7-1* mutants  
180 were able to generate a rosette of almost WT-like appearance. The leaf blades were slightly  
181 smaller and the petioles shorter than in WT (Fig. 1B). It has been observed that a transitory  
182 green stage with photosynthetic activities occurs in *Arabidopsis* embryos starting from the  
183 early torpedo stage (7-9 days after fertilization (daf)) until the end of the maturation (mature  
184 green stage at 23-27 daf) (Allorent et al., 2013). Checking this phase we found in siliques of  
185 heterozygous *pap7-1* mutants both green and white seeds with a segregation ratio of 3:1  
186 indicating that already in homozygous embryos the chloroplast formation is prevented (Fig.  
187 1C). Since these seeds, however, were capable to germinate with no bias in allelic  
188 transmission (3:1 ratio of homozygote mutants), this lack of chloroplast biogenesis appears  
189 to be not essential for proper seed development and maturation. When growing the progeny  
190 of such heterozygous *pap7-1* mutants on sugar-supplemented medium in short-day  
191 conditions under very dim light (approx. 8-12  $\mu$ E WL) homozygous mutant plants developed  
192 a reasonable rosette that was even able to initiate the flowering programme after shifting the  
193 plant container to long-day-conditions (Fig. 1C, D). Architecture and size of the resulting  
194 inflorescence did not exhibit major differences in comparison to green plants as indicated by  
195 control plants grown in the same containers (Fig. 1D). In sum, these observations indicate  
196 that the major photomorphogenic programmes (and hence the action of the corresponding  
197 photoreceptors) are functional in the mutant.

### 198 **Transcript accumulation in albino *pap7-1* plastids**

199 All *pap* mutants analyzed so far display largely reduced accumulation of PEP-dependent  
200 transcripts while NEP-dependent gene transcripts do over-accumulate (Borner et al., 2015;  
201 Pfanschmidt et al., 2015). In all published reports, however, only a few representative



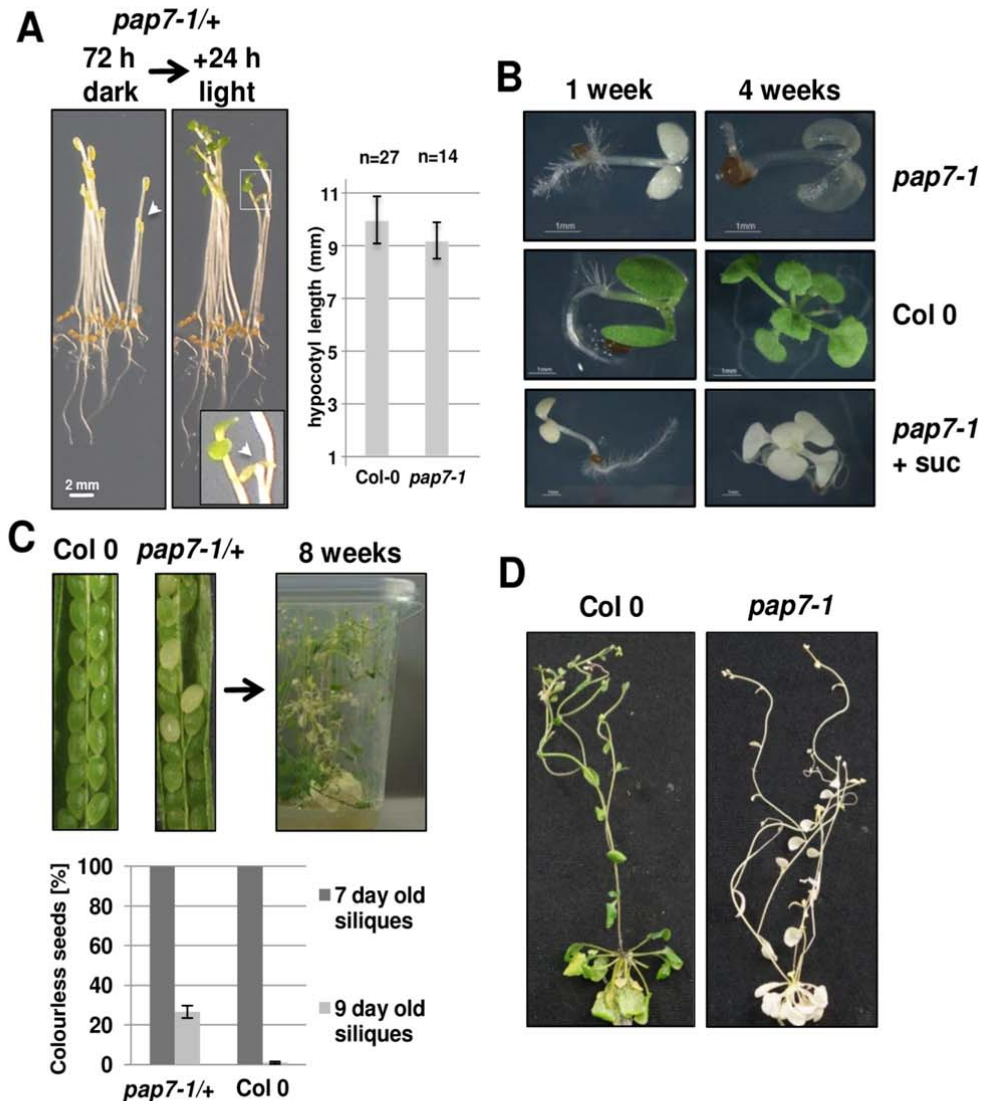


**Figure 1.** Developmental characteristics of the *pap7-1* mutant. A, 72h-dark-grown progeny of a *pap7-1/+* heterozygote subjected to 24h of 20  $\mu$ E white light to trigger photomorphogenesis. White arrowheads indicate a *pap7-1* homozygote mutant before and after subjection to light. Hypocotyl length  $\pm$  standard deviation measured after 72 h of dark growth. Genotypes were assigned after 24 h of light exposure (n= number of measurements). B, Growth of homozygous *pap7-1* seedlings and WT on  $\frac{1}{2}$  strength MS-medium in Petri-dishes without or with (+ suc) sucrose supplementation. C, Impact of *pap7-1* inactivation on chloroplast development during transient embryo greening and seed segregation in siliques of heterozygous *pap7-1* mutants (*pap7-1/+*) in comparison to WT (two left panels). Long-term growth (8 weeks) of the progeny of heterozygous mutants was performed on  $\frac{1}{2}$  strength MS-medium supplemented with 3% sucrose in transparent plastic containers in a short-day light period (right panel). Seed segregation into green and colourless seeds was counted in 7-10 siliques per measurement day (7 or 9 days after fertilization) in WT and *pap7-1/+* mutants (bottom panel). D, Long-term grown plants in rosette stage were put into long-day conditions to induce flowering and photographed at the flowering stage.

202 genes per gene class were investigated. Here, we performed a comparative plastome-wide  
 203 analysis in which we determined the accumulation of all plastidial mRNAs in light-grown

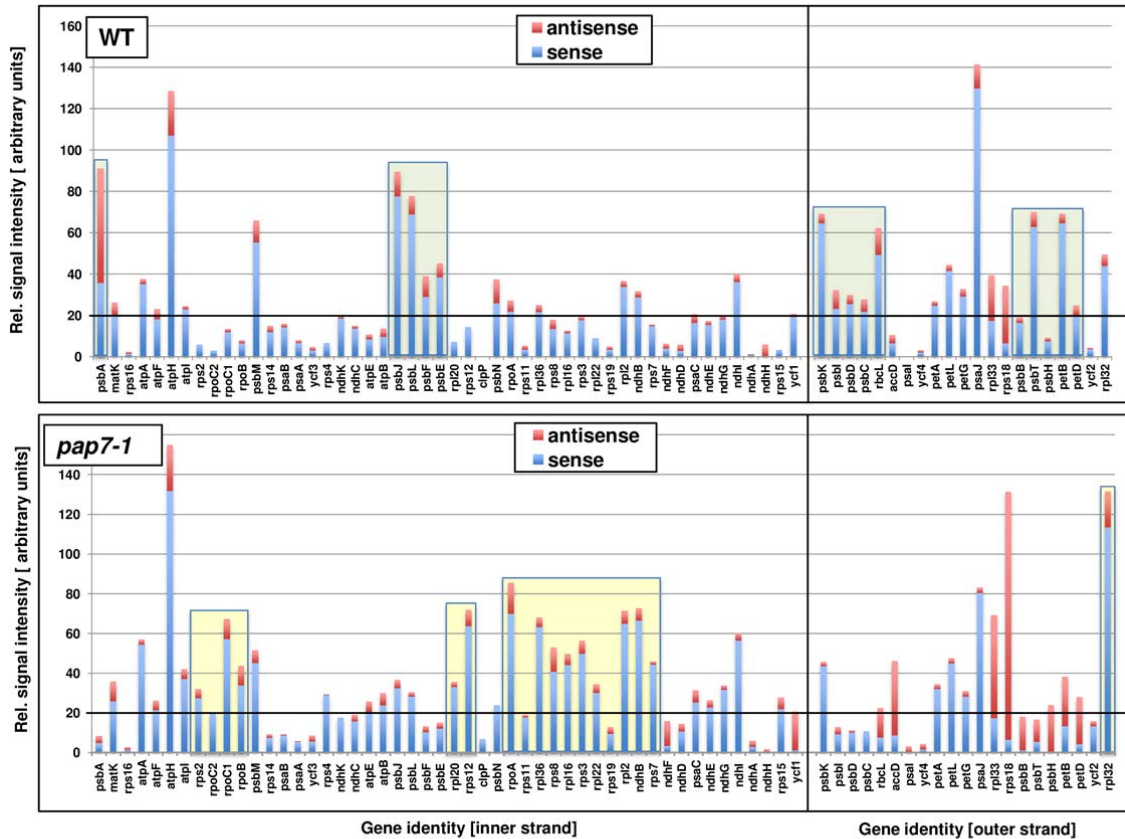


**Figure 2.** Macro-array analysis comparing plastid transcript accumulation in light-grown wild-type and *pap7-1* *Arabidopsis* seedlings. Given is the transcript accumulation in wild-type (top panel) and mutant (bottom panel) seedlings both for sense (blue bars) and anti-sense (red bars) transcripts. Hybridization signals were normalized to the total signal intensity of the membrane and are given as arbitrary units in the left margin. Genes are labeled at the bottom of each panel according to accepted nomenclatures. Sequence of genes corresponds to their organization on the plastome separated between inner strand (left parts) and outer strand of the plastome (right parts). High transcript accumulation of PEP-dependent transcripts in WT is high-lighted by green boxes. High transcript accumulation of NEP-dependent transcripts in the *pap7-1* mutant is high-lighted by yellow boxes.

204 *pap7-1* mutant plants and in WT plants grown in parallel (Fig. 2). To this end we used a  
 205 custom-made macro-array that, in addition to sense RNAs, allowed also the detection of all  
 206 corresponding antisense RNAs (Demarsy et al., 2012). Plastidial antisense RNAs were found  
 207 in *Arabidopsis* to accumulate specifically in early phases of germination and radicle out-  
 208 growth, two developmental steps preceding chloroplast biogenesis (Demarsy et al., 2012).

209 We observed reduced transcript accumulation for many PEP-dependent class 1 genes.  
 210 However, mainly *psb* genes (encoding PSII components) were affected in the mutant (Fig. 2,  
 211 light-green boxes) while for *psa* genes (encoding PSI components) the reduction was found  
 212 to be less pronounced or even not existing. Genes for the cytochrome  $b_6f$  complex (*pet*  
 213 genes) displayed mixed responses ranging from almost none to strong reduction of transcript  
 214 accumulation. In contrast, all class 2 genes (genes with PEP and NEP promoters) displayed  
 215 a stable or even enhanced transcript accumulation in the mutant. This class includes the *ndh*  
 216 genes (encoding components of the NADH dehydrogenase complex), the genes encoding

217 the proteins of the small (*rps*) and large (*rpl*) ribosomal subunits and genes for components  
218 of the ATP synthase (*atp*). Enhanced accumulation could be also observed for class 3 genes  
219 (genes with NEP promoters only) *rpoA* and *rpoB/C1/C2* (encoding the PEP core subunits)  
220 (Fig. 2, yellow boxes), but not for the class 3 genes *ycf1* and *accD*. A general down-  
221 regulation of PEP-dependent genes and a corresponding up-regulation of NEP-dependent  
222 genes as suggested thus cannot be confirmed by our macroarray analysis.

223 These observations were independently supported by the microarray analysis that includes  
224 the full set of plastome located genes. In addition, the microarray also includes all tRNA  
225 genes that are not covered by the macroarray (Supplemental Table 1). These displayed all  
226 strongly reduced accumulation in the *pap7-1* mutant line suggesting that they are transcribed  
227 by PEP. This is in agreement with results obtained in a recent study on *pap* mutants of maize  
228 (Williams-Carrier et al., 2014).

229 Antisense RNA accumulation for most genes displayed no major differences between WT  
230 and *pap7-1* mutant plants. However, we observed specific over-accumulation of antisense  
231 transcripts for the *psbB/psbT/psbH/petB/petD* operon, *rpl33* and *rps18* genes and the two  
232 genes *ycf1* and *accD* (encoding import machinery subunit TIC214 and the  $\beta$ -subunit of the  
233 acetyl-CoA carboxylase complex, respectively) (Fig. 2). This differential accumulation  
234 suggests that antisense production is not just a concomitant by-product of read-through  
235 transcription, but that a distinct unknown mechanism is at its origin.

236 In summary, our macro-array experiment uncovered that the disturbance in PEP activity  
237 does not cause gene-class specific transcription changes but rather many gene-specific  
238 effects suggesting a much more complex transcription regulation in arrested albino plastids  
239 than current models anticipate.

240

## 241 **Separation of light- and plastid-dependent gene regulation during** 242 **photomorphogenesis by trilateral differential gene expression profiling**

243 Chloroplast biogenesis is embedded into the general photomorphogenic programme of  
244 seedling development which strongly impedes a clear distinction of light-, development- and  
245 plastid-dependent signaling (Lopez-Juez et al., 1998; Lopez-Juez, 2007). However, since  
246 illuminated *pap7-1* mutants develop normally on sucrose-supplemented media (Fig. 1) (Gao  
247 et al., 2011; Steiner et al., 2011) indicating that chloroplast biogenesis can be separated from  
248 photomorphogenesis, we used it as a tool to separate the gene groups regulated by either  
249 light or plastid developmental stage. To this end we performed genome-wide differential  
250 gene expression profiling in *Arabidopsis* by microarray hybridization. In order to unravel truly

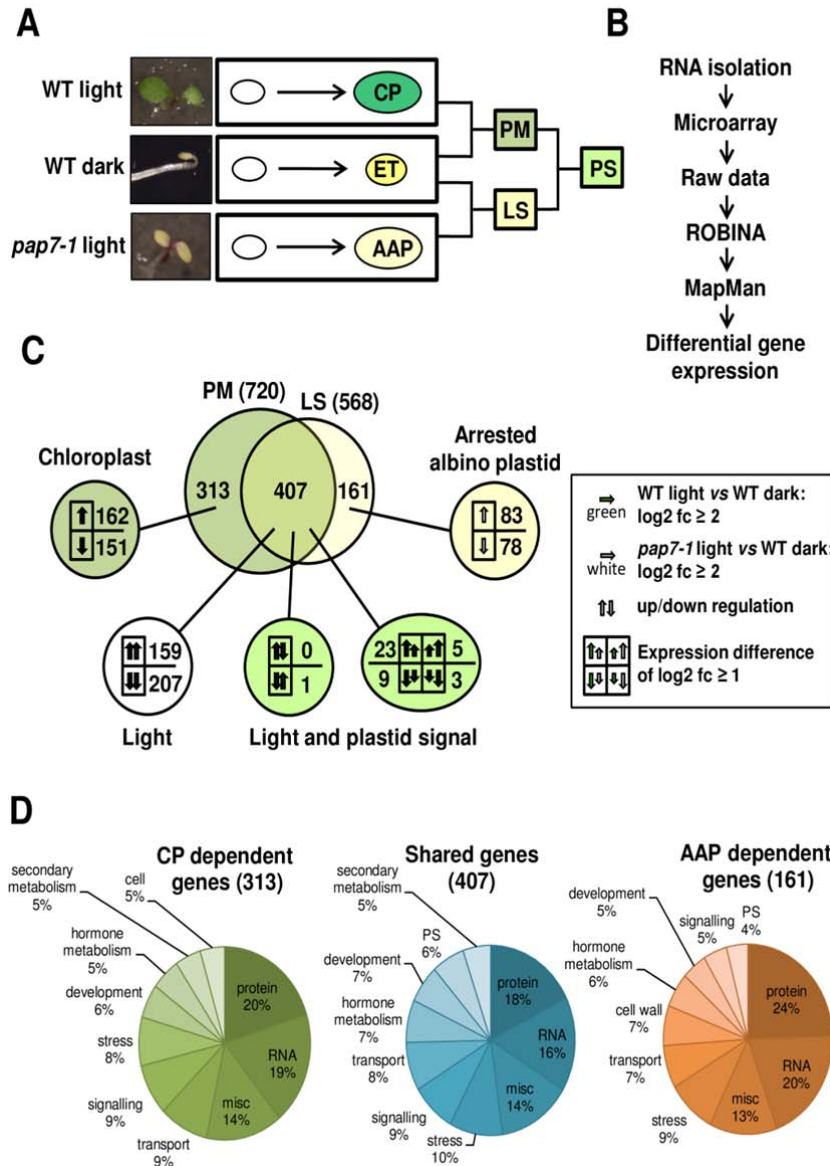


**Figure 3.** Identification of gene modules responsive to light and/or biogenic plastid signals. A, Strategy for differential expression profiling of 4-5-day-old *Arabidopsis* seedlings in wildtype (WT) and *pap7-1* mutants (*pap7-1*). Left panel displays photographs of seedlings with representative phenotypic appearance. The right panel indicates the corresponding developmental transition of the plastids in each of these seedlings. White small ovals represent undifferentiated pro-/eoplasts from seeds. Upon illumination they develop into green chloroplasts (CP) in WT (WT light) or arrested albino plastids (AAP) in *pap7* mutants (*pap7-1* light). Growth in the dark leads to development of yellow etioplasts (ET) in WT (WT dark). Analysis of differences between expression profiles in these plant samples (indicated by brackets) identify genes for photomorphogenesis (PM), for plastid-independent light signaling (LS) and for plastid signalling (PS) (for details see text). B, Flow diagramme of bioinformatic analysis done with primary expression data from the microarray analysis. C, Detailed comparison of differentially expressed genes (indicated by numbers) within the PM and LS expression modules according to their direction of expression change (indicated by arrows). Only genes exceeding a threshold of  $\log_2 \text{fc} \geq 2$  were taken into analysis. Genes found in both modules were further separated according to their direction and degree of gene expression change. Arrows of different size but same direction indicate genes that display the same direction of expression change but with a difference of at least  $\log_2 \text{fc} \geq 1$ . Green arrows: Expression change in WT. White arrows: Expression change in *pap7-1* mutants. For more details see legend box. D, Proportional distribution of genes within the different gene groups defined in Fig. 3C according to their functional association within MapMan bins.

252 profiling including light grown *pap7-1* mutant seedlings (*pap7-1*-light, containing white  
253 plastids), light-grown WT seedlings (WT-light, containing chloroplasts) and dark-grown WT  
254 seedlings (WT-dark, containing etioplasts), all at the two-cotyledon-stage (Fig. 3A). We  
255 performed a supervised analysis of the expression data using the MapMan tool (Usadel et  
256 al., 2005) and an unsupervised analysis by performing a weighted gene expression network  
257 analysis (WGCNA) using gene ontology (GO) groups in order to combine the advantages of  
258 both gene categorization tools (Klie and Nikoloski, 2012).

259 In our supervised strategy we assumed that a WT-light to WT-dark comparison reveals  
260 expression changes controlled by the photomorphogenic program (PM, Fig. 3A). This should  
261 identify all genes activated or inactivated by light and plastid signals. A parallel comparison of  
262 *pap7-1*-light and WT-dark should identify genes being regulated only by light while the  
263 developmental status of the plastid is negligible (light signaling, LS, Fig. 3A) since both  
264 samples do not develop chloroplasts. Subsequent comparison of the significantly regulated  
265 gene groups identified in PM and LS then should identify genes specifically regulated by  
266 light, by plastid stage or by both (PS, Fig. 3A).

267 Significantly regulated genes in the data sets were identified (Supplemental Table 1) and  
268 were imported into the MapMan visualization tool (Fig. 3B, Supplemental Figure 1). As  
269 expected, the PM data set revealed large genome-wide changes known to be characteristic  
270 for the photomorphogenic program (Ma et al., 2001). This included a massive up-regulation  
271 of genes for photosynthesis, energy metabolism and tetrapyrrole biosynthesis as well as  
272 sulfate reduction and a great number of other biosynthetic pathways (Supplemental Figure  
273 1A). In the LS data set we observed an impact on mostly the same gene groups and with  
274 similar strength indicating that the light-regulation in the *pap7-1* mutant works in a  
275 comparable manner as in WT (Supplemental Figure 1B). Direct comparison of *pap7-1*-light  
276 versus WT-light gene expression profiles demonstrated only limited differences  
277 (Supplemental Figure 1C) indicating that the gene regulation in the light-grown *pap7-1*  
278 mutant resembles much more to that of light-grown than to dark-grown WT. This indicates  
279 that the lack of functional chloroplasts in the *pap7-1* mutant exerts only a minor impact on  
280 light-regulated gene expression networks.

281 The quality of the expression profiles obtained in the microarray approaches was tested by  
282 quantitative RT-PCR of selected genes being representative for different expression classes  
283 found. To this end RNA was isolated from identically, but independently grown plant samples  
284 from WT and *pap7-1* mutants. As a further independent control for the arrested plastid  
285 development another *pap* mutant, *pap6-1*, was used (Gilkerson et al., 2012). All genes tested  
286 in the qRT-PCR displayed highly reproducible expression data (correlation factors above 0.9)  
287 when compared to the corresponding data obtained from the microarrays (Fig. 4,

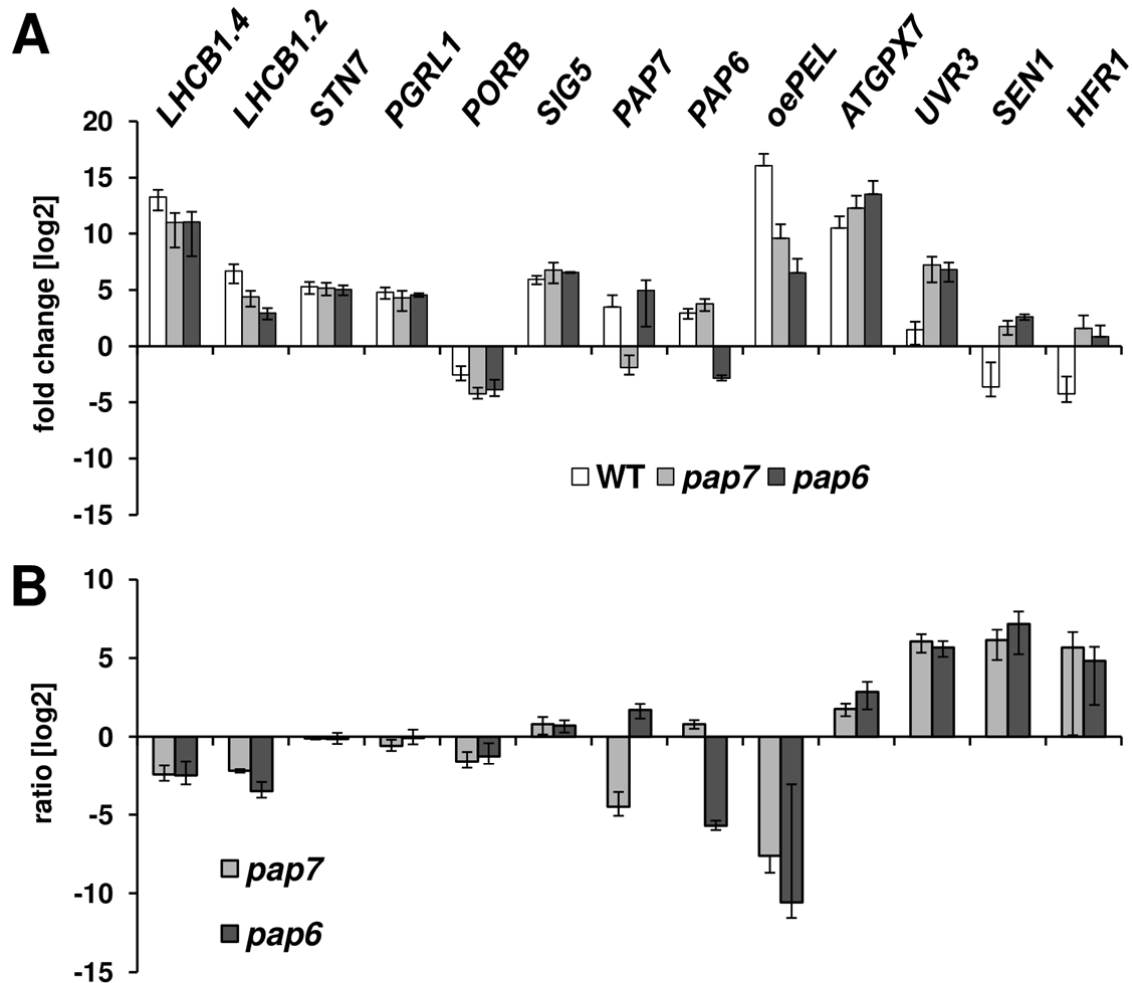


**Figure 4.** Expression profiles of selected genes from the microarray analysis tested by qRT-PCR. (a) Expression changes of genes representative for distinct expression classes in WT-light, *pap7-1* and *pap6-1* mutants compared to WT-dark. Genes for proteins Lhcb1.4, Lhcb1.2 and oePEL (light harvesting complex II proteins 1.4 and 1.2, “overexpression leads to pseudo-etiolation in light”) represent genes displaying a reduced light induction in *pap7-1* when compared to WT. Genes encoding proteins STN7, PGRL1a and SIG5 (state transition kinase 7, PGR5-like protein 1a, sigma factor 5) represent genes displaying no effect of *pap7-1* on light induction, while the gene for PORB (protochlorophyllide oxidoreductase B) represents an example for strong light repression both in WT and *pap7-1* mutant. The genes for ATGPX7 and UVR3 (glutathione peroxidase 7 and (6-4) DNA photolyase) were used as examples displaying light induction in WT and further promotion in *pap7-1*. Genes for SEN1 and HFR1 (senescence-associated protein DIN1 and the transcription factor Long Hypocotyl after far-red 1) represent genes displaying repression in WT but promotion in the mutant. As additional genetic control *pap6-1/fln1* (defective in the gene for a phospho-fructokinase like 1 protein) was used in order to detect potential mutation-specific responses. Expression of both *pap* genes was tested in all RNA samples as further control. (b) Difference in expression change between light grown WT and the *pap7-1* and *pap6-1* mutants. Negative values indicate lower expression, positive values higher expression than in WT. Data given represent means of three independent experiments. Primers used are given in Supplemental File 12.

288 Supplemental Figure 2). Furthermore, the expression data in the two different *pap* mutants  
 289 displayed a remarkable low variation (Fig. 4) indicating that the observed expression profiles  
 290 in the mutant background are robust and likely representative not only for *pap7-1* but also for  
 291 other *pap* mutants.

**293 Identification of gene groups responding either to light or to biogenic plastid signals**

294 Next, we performed a more detailed analysis of the various regulated gene groups. In order  
295 to restrict the analysis to strongly regulated genes we introduced a threshold of log<sub>2</sub> fold  
296 change (fc) ≥ 2 for definition of significantly regulated genes (in total 881 genes). Identities  
297 and expression changes of these genes are given in Supplemental Table 2. 720 genes in the  
298 PM data set and 568 genes in the LS data set met this criterion (Fig. 3C). 407 genes were  
299 identified in both data sets with a majority being regulated in the same direction in both  
300 conditions (Fig. 3C, 159 up-regulated and 207 down-regulated genes). These 366 equally  
301 regulated genes were not influenced by the developmental state of the plastid but by  
302 illumination only. They, thus, represent plastid-independent, light-regulated genes. Only 41 of  
303 the 407 genes displayed either opposite (1 gene) or different strength in their regulation  
304 where we regarded only differences of at least log<sub>2</sub> fc ≥ 1 as significant. These genes appear  
305 to be partly affected by both, plastid stage and light. The largest group (23 genes) displayed  
306 up-regulation in WT-light *versus* WT-dark, but significantly less up-regulation in *pap7-1*-light  
307 *versus* WT-dark. This expression pattern corresponds to the regulation mode attributed to  
308 the classical definition of a plastid signal that causes a lower accumulation of light-induced  
309 nuclear gene transcripts when chloroplast development is inhibited by chemical or genetic  
310 means (Pfannschmidt 2010).

311 In addition, we identified 313 genes that were exclusively up- (162) or down- (151) regulated  
312 only when chloroplast biogenesis occurred (CP-dependent genes, Fig. 3). These genes,  
313 thus, may either cause chloroplast biogenesis or are related to specific functions exerted by  
314 this fully developed plastid type such as retrograde redox regulation from photosynthesis.  
315 Interestingly, we identified 161 genes that displayed exclusive up- (83) or down- (78)  
316 regulation only in the presence of the arrested albino plastid (AAP-dependent genes, Fig. 3).  
317 These genes are likely regulated because of the missing chloroplast biogenesis or function  
318 (i.e. photosynthesis or connected biosynthesis pathways). Both developmental plastid stages  
319 apparently send distinct, light-independent signals to the nucleus that either repress or  
320 enhance separate sets of genes. Because of their light-independency these signals are not  
321 identical with the “classical” plastid signal and imply the existence of plastid-type specific  
322 positive and negative signals not yet defined by current models of retrograde signaling.

323 In total, 41.5% of the 881 strongly regulated genes appear to be light-regulated, 4.6% are  
324 regulated by combined light and plastid signals and 53.8% (corresponding to 474 genes) are  
325 regulated by plastid signals only (CP and AAP). Decreasing the threshold for significant  
326 regulation to log<sub>2</sub> fc ≥ 1 identified 3658 regulated genes, which is roughly four times more

327 than with  $\log_2 fc \geq 2$  as threshold (Supplemental Table 3). In this larger group 46.4% of the  
328 genes appear to be light-regulated, 3.9% are regulated by light and plastid signals and  
329 49.5% are regulated by plastid signals only (Supplemental Figure 3). Thus, enlargement of  
330 the number of investigated genes did not result in major relative changes between the three  
331 regulation modes indicating that the arbitrarily chosen thresholds did not produce a bias for  
332 specific regulation pattern. The inclusion of dark-grown plants as additional reference point  
333 instead of doing a direct comparison of WT-light and *pap7-1*-light, thus, provides a much  
334 more precise separation of plastid- and light-regulated genes. Both factors control very  
335 distinct sets of genes and the over-lap between the two signaling pathways/expression  
336 networks appears to be very limited.

337

338 **Among photosynthesis-associated nuclear genes only *LHCB* genes are affected by**  
339 **plastid signals in *pap7-1***

340 The CP-, light- and AAP-dependent genes were finally sorted according to their functional  
341 categories (MapMan bin) (Fig. 3D). The majority of functional categories were identical for all  
342 three groups comprising the MapMan bins “protein”, “RNA”, “stress”, “transport”, “signaling”,  
343 “development” and “hormone metabolism”. Interestingly, the group of CP-dependent genes  
344 did not include “photosynthesis genes”, while the group of AAP-dependent genes did not  
345 include the bin “secondary metabolism”, but instead the bin “cell wall”. The large overlap in  
346 functional categories, however, is not reflected at the level of individual gene identities (Table  
347 S1) and our analysis clearly demonstrates that each gene group represents a distinct set of  
348 regulated genes (see also results from WGCNA).

349 The lack of photosynthesis genes in the CP-dependent group was surprising with respect to  
350 the notion that photosynthesis associated nuclear genes (PhANGs) are considered to be a  
351 prime target for plastid signals during biogenic control. We, therefore, analysed these genes  
352 separately and compared their relative expression changes in the PM and LS data sets (Fig.  
353 5A). In WT-light *versus* WT-dark 76 genes exhibited a light-induced expression increase of  
354  $\log_2 fc \geq 1$ . 93 photosynthesis genes (including all plastome localized genes) displayed  
355 expression variations that remained below this threshold suggesting that they are not or just  
356 mildly affected by light. Only 15 genes exhibited a strong light induction of  $\log_2 fc \geq 2$ . The  
357 top five of these genes all encode proteins of the light-harvesting complex of PSII (*LHCB*)  
358 (framed in Fig. 5A). In the *pap7-1*-light *versus* WT-dark comparison we observed a similar  
359 expression profile for photosynthesis genes. Here, 62 genes exhibited light-induced  
360 expression of  $\log_2 fc \geq 1$  and 11 genes displayed expression changes of  $\log_2 fc \geq 2$ . Ten of  
361 these genes were also found as top-regulated genes in WT. However, we observed that



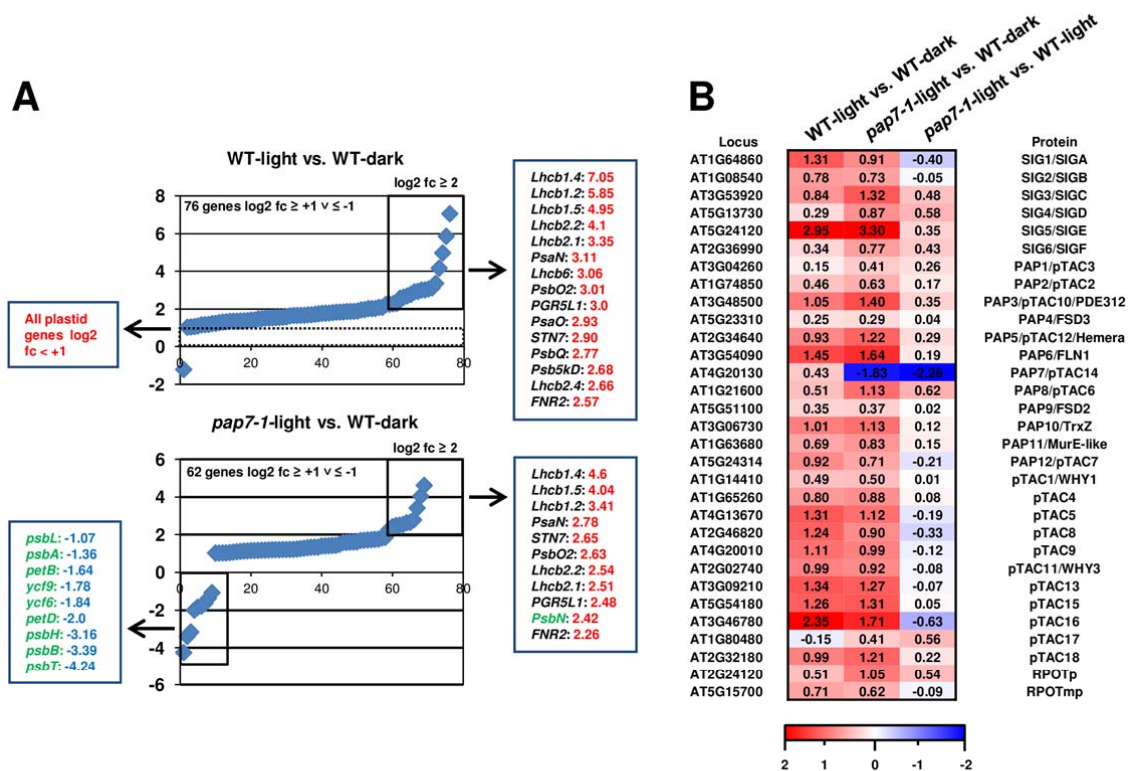


**Figure 5.** Light-induced expression changes of genes for photosynthesis and plastid transcription. A, The graphs display the expression values of significantly light-affected photosynthesis genes ( $\log_2 \geq 1$ ) detected by comparison of expression profiles WT-light versus WT-dark (top graph) and *pap7-1*-light versus WT-dark (bottom graph). From the 169 photosynthesis genes present in the corresponding MapMan bin 72 and 62 genes, respectively, exhibited an expression change of at least  $\log_2 \geq 1$ . In the WT-light versus WT-dark comparison all plastid genes remained below this threshold. Genes exceeding an expression change of  $\log_2 \geq 2$  were boxed in the graph and listed in a panel aside. Nuclear encoded genes are given in black, plastid encoded genes are given in green. The difference in the expression change of a particular gene that occurs between the top and the bottom panel reflects the plastid influence on its expression. Strongly down-regulated genes in *pap7-1*-light versus WT-dark ( $\log_2 \geq -1$ ) are given in a left box. B, Expression changes for all 31 nuclear genes encoding components of the plastid gene transcription machinery in WT and *pap7-1*. The respective comparisons are indicated in the top panel, gene identities in the left and protein identities in the right panels. Given values represent log 2 fold changes, a corresponding color code is depicted at the bottom level.

362 specifically *LHCB* genes displayed significant less accumulation in *pap7-1* compared to WT  
 363 while all other genes remained fairly constant. Comparable results were obtained in the  
 364 independent qRT-PCR controls (Fig. 4). This reduced expression can be attributed to the  
 365 impact of biogenic signals from the arrested albino plastid. In addition, we observed also nine  
 366 significantly down-regulated genes in this comparison, all of them being plastome-localized  
 367 (Fig. 5A). This confirms the observation using the MapMan visualization (Supplemental  
 368 Figure 1) in which inhibition of chloroplast development had only limited impact on the overall  
 369 nuclear gene expression profile. We conclude that inhibition of chloroplast development in

370 the *pap7-1* mutant represses specifically plastome-localized photosynthesis genes and of a  
371 small set of nuclear *LHCB* genes while all other PhANGs are either not affected or just mildly  
372 attenuated.

373 Another interesting question was whether or not other nuclear genes for components of the  
374 plastid transcription machinery were affected in their expression by the repressed PEP  
375 activity in *pap7-1* plastids. We, therefore, analyzed the expression data of genes for all sigma  
376 factors, PAPs, PTAC components and for NEP. The majority of these components displayed  
377 light induction in WT when compared to the dark control (Fig. 5B). This is in accordance with  
378 earlier bioinformatic analyses. The observed regulation patterns were largely maintained in  
379 the mutant with only minor deviations from the WT indicating that the developmental state of  
380 the plastid has also no significant impact on the expression of these genes while light  
381 appears to be a dominant regulator even in the mutant. The functional PEP deficiency, thus,  
382 does not exert a retrograde repressive control of other nuclear encoded PEP or NEP  
383 components.

384

#### 385 **Weighted gene expression correlation network analysis (WGCNA)**

386 The supervised analysis (Fig. 3) used pre-settings based on assumptions drawn from  
387 literature and our own experiences. In order to avoid any unwanted bias we performed an  
388 additional un-supervised analysis of the gene expression data sets employing a weighted  
389 gene expression correlation network analysis (WGCNA) (Supplemental Figure 4). As in our  
390 supervised analysis the cluster analysis of the expression data revealed a much closer  
391 correlation between *pap7-1*-light and WT-light samples than between *pap7-1*-light and WT-  
392 dark samples (Fig. 6). Nevertheless, the gene expression profiles of *pap7-1*-light and WT-  
393 light samples displayed a number of specific differences. In total, six significant gene  
394 expression modules could be identified by WGCNA within the data set (Supplemental Figure  
395 4). These modules describe characteristic similarities and differences between the three  
396 plant samples and largely correspond to the groups defined in the supervised differential  
397 analysis. Since the unsupervised analysis did not include expression thresholds, it, however,  
398 covered much larger gene numbers. The identified expression modules divide into two  
399 groups (Supplemental Figure 4B). Group1 comprises three modules (modules blue, yellow  
400 and green) in which two samples are highly similar while the third one is opposing. Group 2  
401 comprises three modules (modules turquoise, brown and red) in which two samples are  
402 opposing while the third one is in an intermediate state between the two other.

403 Genes in module “blue” (in total 1838 genes) display highly similar expression in *pap7-1* light  
404 and WT light samples and an opposing expression in WT dark. The dominant regulating

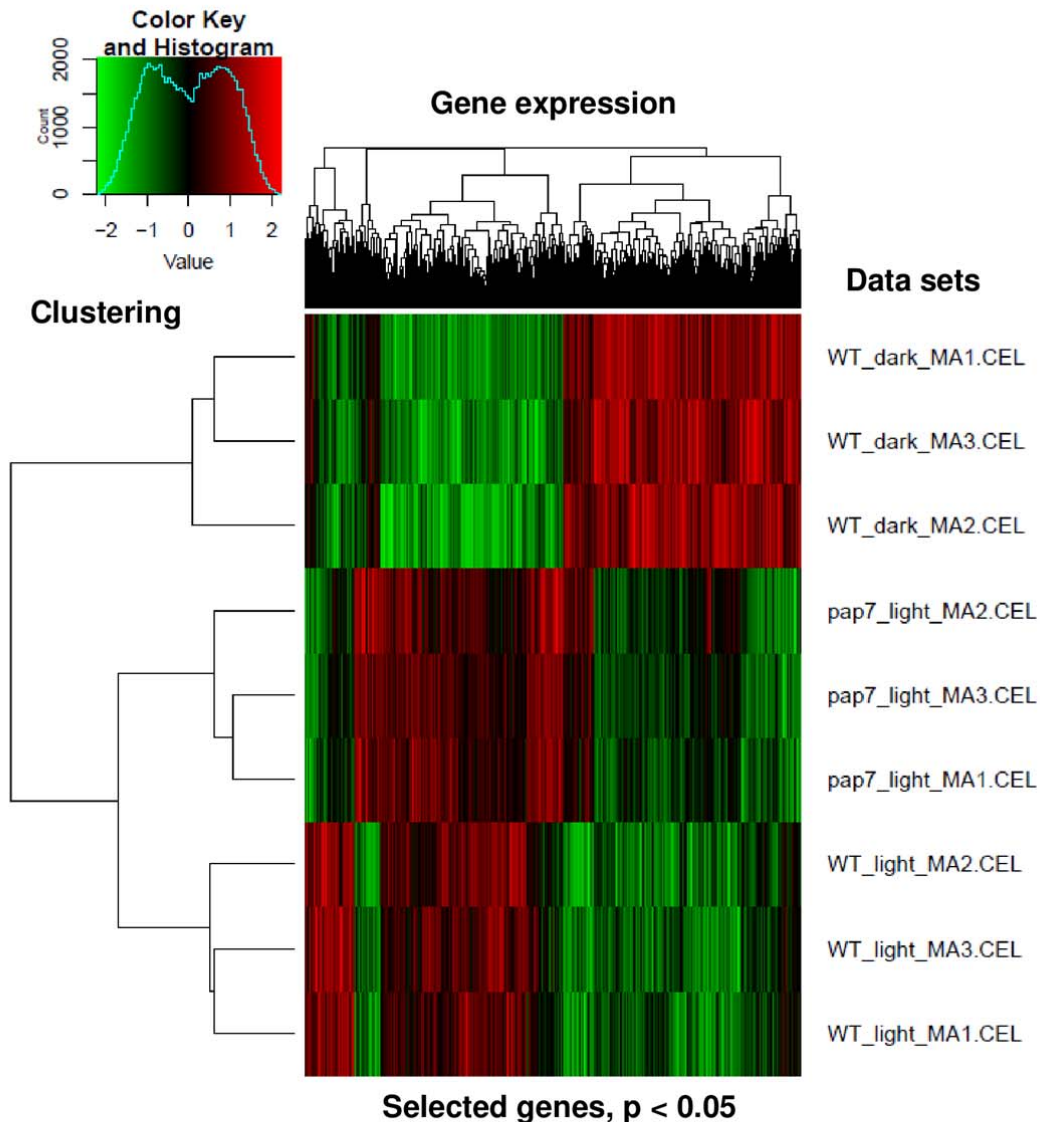


**Figure 6.** Cluster analysis of genes differentially regulated in the three growth set-ups as defined by ANOVA. Genes displaying a FDR of  $< 0.05$  were included. The right margin identified the data sets from the microarray analysis, the left margin indicates a cladogram defining the correlation in gene expression profiles between them. On top clustering of gene groups according to their expression is indicated. Diagramme in top left corner gives the color key and numbers of genes with corresponding gene expression values. Red: Up-regulation. Green: Down-regulation.

405 factor in this module, thus, is the light while the plastid state appears to play no or a very  
 406 minor role. Module “blue”, therefore, covers the light-regulated genes. Genes in module  
 407 “yellow” (in total 769 genes) display highly similar expression in *pap7-1* light and WT dark  
 408 samples and an opposing expression in WT light. The dominant regulating factor here is the

409 plastid state while light appears to have no major impact. Module “yellow”, thus, covers  
410 genes under plastidial regulation that is exerted from a normally developed chloroplast.  
411 Genes in module “green” (in total 671 genes) display a highly similar expression in WT light  
412 and WT dark samples and an opposing expression in *pap7-1* light. Light appears to be of no  
413 importance for the regulation of these genes, but the arrested plastid development and the  
414 genetic background of the mutant. Module “green”, therefore, covers genes that are mis-  
415 regulated because of the disturbance in plastid development and the *pap7-1* protein  
416 deficiency. The expression profiles of the genes covered by these three modules correspond  
417 to those in the three gene groups defined in our supervised analysis (Fig. 3C) and provide  
418 independent analytical confirmation for the correctness of our selection criteria.  
419 Understanding and interpretation of the modules in group 2 appeared to be much more  
420 difficult as the intermediate expression profiles in each module prevent an identification of the  
421 dominant regulating factor. Gene groups defined by these modules, thus, are likely under  
422 multi-factorial control and were, therefore, excluded from further analysis.

423 We analyzed the three gene modules for enriched GO groups (Supplemental Figures 5-7)  
424 and indicated most important GO groups with respect to the mutant phenotype below. Light-  
425 regulated genes in module “blue” included the GO groups for “Photosynthesis”, “Isoprenoid  
426 biosynthesis”, “Tetrapyrrole biosynthesis” and for “Anatomical structure and morphogenesis”  
427 (Fig. 7A). All these gene groups are apparently activated by light without displaying a major  
428 impact of the developmental state of the plastid. Like in the supervised analysis PhANGs  
429 occur under the light-regulated gene groups supporting the notion that the impact of the  
430 plastid stage on the expression of this gene group is very limited. Chloroplast-regulated  
431 genes in module “yellow” (Fig. 7B) contained GO groups for “Cellular metabolic processes”,  
432 “Photoperiodism and flowering”, “Fatty acid beta oxidation”, “Protein localization to  
433 peroxisome”, “Glucosinolate biosynthetic process” and “Indoleacetic acid metabolic  
434 processes”. While the first four groups appear to be repressed, the latter two are mainly  
435 activated by the presence of functional chloroplasts. Finally, in the *pap7-1*-regulated module  
436 “green” (Fig. 7C) we found GO groups for “Nitrogen compound metabolism processes”,  
437 “Circadian rhythm” and “Reproductive system development”. These gene groups were either  
438 activated or stayed active upon the genetic arrest of chloroplast biogenesis. Our triplicate  
439 analyses, thus, describe distinct gene sets that are specifically targeted by the three factors  
440 light, chloroplasts and arrested albino plastids both in positive and negative manner.

441

442

443

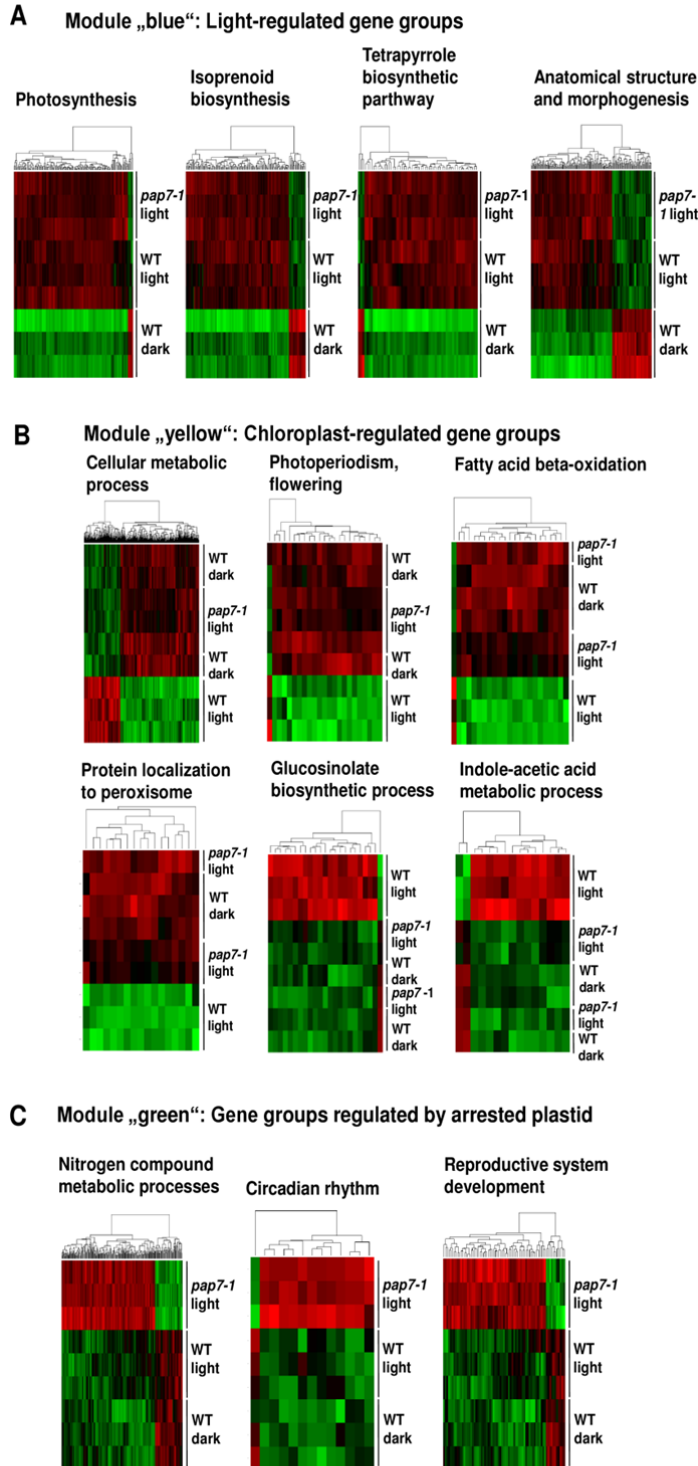


**Figure 7.** GO groups of differentially expressed gene sets within the gene modules identified by WGCNA. A, Gene module „blue“ with four major gene groups regulated by light. B, Gene module „yellow“ with six major gene groups regulated by the chloroplast. C, Gene module „green“ with three major gene groups specifically regulated by the arrested plastid. Genes displaying a FDR of < 0.05 were included. On top of each heat map the selected GO group is given, underneath a clustering of the genes in this group according to their expression is indicated. The right margin identifies the data sets from the microarray analysis. Red: Up-regulation. Green: Down-regulation. For further gene groups see Supplemental Files 8-10.

445 Our plastome- and genome-wide gene expression analysis in the *pap7-1* mutant provides  
446 the first detailed view of the disturbances occurring at the transcript level of this mutant. This  
447 revealed interesting and unexpected facts that help to better understand the causes for the  
448 albinism in this mutant. In addition, the obtained data provide important novel clues for our  
449 understanding of other *pap* mutants as well as retrograde biogenic signals and their target  
450 genes.

451

## 452 **Impact of *pap7-1* deficiency on plastid gene expression**

453 Elucidation of the plastid transcriptome in the *pap7-1* mutant uncovered that many PEP-  
454 dependent class I transcripts displayed only low accumulation while NEP-dependent *rpo*  
455 transcripts exhibited enhanced accumulation (Fig. 2). This is in coincidence with earlier  
456 reports. However, we observed significant differences between *psa* and *psb* gene groups  
457 suggesting differential effects on class I transcription. In addition, NEP-dependent *ycf1* and  
458 *accD* gene transcripts did not over-accumulate as *rpo* transcripts, but exhibited clearly  
459 reduced transcript accumulation (Fig. 2). Furthermore, class II transcripts revealed largely  
460 WT-like accumulation in the mutant (Fig. 2). These effects cannot be reconciled with the  
461 current model of plastid transcription in albino plastids of *pap* mutants which assumes a  
462 general inactivation of PEP activity while the NEP activities are up-regulated. Instead these  
463 data imply differential and gene-specific effects on transcription activities in the albino  
464 plastids. Since all class I transcripts did accumulate to a certain degree in *pap7-1* plastids it  
465 is likely that these arise from a basal activity of the PEP core-complex. Such a basal activity  
466 was identified in etioplasts of mustard and was shown to be able of faithful promoter  
467 recognition using sigma factors, however, in a different manner than the corresponding  
468 activity from chloroplasts (Eisermann et al., 1990; Tiller and Link, 1993; Pfannschmidt and  
469 Link, 1994). This scenario could provide a realistic explanation for the observed  
470 transcriptome in the *pap7-1* mutant plastids and suggest that the gene expression  
471 mechanisms in the albino plastids are likely arrested in a stage similar to etioplasts.  
472 Alternatively, the residual class I transcripts may arise from read-through transcription  
473 performed by NEP enzyme activities; however, such a model would lack an explanation for  
474 differential gene group transcription. Regardless of their origin, the residual class I transcripts  
475 apparently are not sufficient to elicit the formation of a photosynthetic apparatus suggesting  
476 the involvement of additional constraints for the chloroplast formation.

477 One such constraint could be the enhanced antisense transcript accumulation in the mutant  
478 which was observed notably for the *psbB/T/H/petB/D* operon, the *rpl33/rps18* operon and the  
479 *ycf1* and *accD* genes (Fig. 2). As this effect appears to be rather gene-specific it likely does

480 not represent just an arbitrary accumulation of read-through transcription of the respective  
481 opposite strand of the plastome. Mechanistically, one could expect that enhanced antisense  
482 transcript accumulation interferes with translation efficiency of the corresponding sense  
483 transcript due to duplex formation as it was suggested for the plastid *psbT* gene (Zghidi-  
484 Abouzid et al., 2011). This would provide a gene-group-specific mechanism that could  
485 prevent the formation of functional photosystem II and Cytb<sub>6</sub>f complexes. Whether this  
486 antisense production is based on a specific transcription event will be an interesting field of  
487 future research.

488 Our microarray analysis of *pap7-1* RNA samples indicated a strongly reduced accumulation  
489 of most plastidial tRNAs (Supplemental file 1). This is in agreement with a recent study  
490 performed in several maize *pap* mutants proposing that PEP activity has a major role in the  
491 expression of plastidial tRNAs (Williams-Carrier et al., 2014). Reduction in plastid tRNA  
492 accumulation restricts plastid translation as the tRNA molecules transfer the amino-acids.  
493 Furthermore, since the tRNA<sup>E</sup> is the precursor of amino-levulinic acid (ALA), tetrapyrrole  
494 biosynthesis and the generation of chlorophylls might be severely affected.

495 In sum the differential accumulation of gene-specific transcripts of all classes implies the  
496 existence of specific, yet unknown, transcription events in the arrested albino plastids  
497 suggesting a more defined and diversified division of labor between the PEP and NEP  
498 enzymes during early steps of chloroplast biogenesis than current models propose.

#### 499 **Retrograde control of nuclear gene expression by biogenic plastidial signals**

500 A major improvement of our study when compared to earlier work in this field arose from our  
501 experimental set-up that included dark-grown WT plants as additional reference point.  
502 Inclusion of homozygous *pap7-1* mutants grown in the dark as further control was not  
503 feasible as homozygous mutant seedlings in this stage remain macroscopically  
504 indistinguishable from WT or heterozygous mutants (Fig. 1A). Discrimination between WT  
505 and mutant genotypes at this stage would be technically possible only at the molecular level  
506 of individual seedlings exacerbating largely the harvest of sufficient material for RNA  
507 preparation. The indistinguishability of dark-grown homozygous mutants is in accordance  
508 with our working hypothesis that the mutation becomes effective only under illumination while  
509 it does not affect the skotomorphogenic programme. Consequently, segregation of the  
510 progeny of heterozygous *pap7-1* mutant plants becomes macroscopically visible only in the  
511 light when the transition towards chloroplasts is arrested. Nevertheless the trilateral  
512 expression profiling allowed us for defining unambiguously distinct gene sets responding  
513 specifically to i) light, to ii) chloroplast signals and to iii) signals from arrested albino plastids.  
514 This distinction is impossible by a simple bilateral mutant-WT comparison in the light as this

515 provides only the relative differences between the two conditions. The impact of light in each  
516 of them requires the additional comparison with the dark control which then reveals whether  
517 light has a promoting, inhibiting or no effect and allows finally for the distinction between  
518 retrograde and light control.

519 The three gene modules identified by our approach contain both activated and repressed  
520 genes, thus, implying the existence of retrograde biogenic signals that are of either positive  
521 or negative nature. Since the gene sets regulated by chloroplasts and arrested plastids are  
522 different it is likely that the controlling signals are transmitted via separate pathways.  
523 Whether these are fully independent from each other or whether they do mutually exclude  
524 each other remains to be investigated. The question whether a weaker nuclear gene  
525 expression indicates the action of a negative signal or the missing action of a positive signal  
526 has been debated in the past (Pfannschmidt, 2010; Terry and Smith, 2013; Hills et al., 2015).  
527 A recent study (Page et al., 2017) and our data presented here indicate that the action of  
528 both, positive and negative signals, needs to be considered in current models.

529 The phenotypic analysis (Fig. 1) revealed that despite chloroplast deficiency the general  
530 photomorphogenic programme in the *pap7-1* mutant appears to be operational as long as an  
531 external carbon source is available. Older mutant plants generate a complete albino rosette  
532 that is comparable to those of dark-grown mutants with constitutively active phytochromes  
533 (Su and Lagarias, 2007) confirming that general plant development and chloroplast  
534 biogenesis represent largely separate processes. Even the initiation of the flowering  
535 transition was found to be functional, which corresponds to observations reported for *rpo*  
536 deletion mutants of tobacco (De Santis-Maclossek et al., 1999). We thus assume that  
537 illumination activates the photoreceptor systems in both WT and *pap7-1* mutant seedlings in  
538 the same manner suggesting that synthesis and action of the photoreceptors (including their  
539 chromophores) are fully functional in the albino mutant.

540 This explains the similarity of the expression profiles of light-grown WT and *pap7-1* mutants  
541 (Supplemental Figure 1) including the expression of the corresponding light-regulated gene  
542 module (module “blue”) (Fig. 8). The module contains the GO groups for isoprenoid and  
543 tetrapyrrole biosynthesis (Fig. 7) that produce important precursor for primary products such  
544 as carotenoids, chlorophylls, haem, phytychromobilin, plastoquinones or different plant  
545 hormones (Pulido et al., 2012). Both biosynthesis pathways provide essential metabolites for  
546 plant metabolism and development and, therefore, are likely active in the albino plastids with  
547 the apparent exception of Chl biosynthesis. For the same reasons the GO group for  
548 morphogenesis and anatomical structure (Fig. 7) may appear in this module because it is  
549 part of the light-initiation of photomorphogenesis. Unexpectedly, however, was the  
550 identification of PhANGs that, in contrast to general assumptions, did not exhibit any major



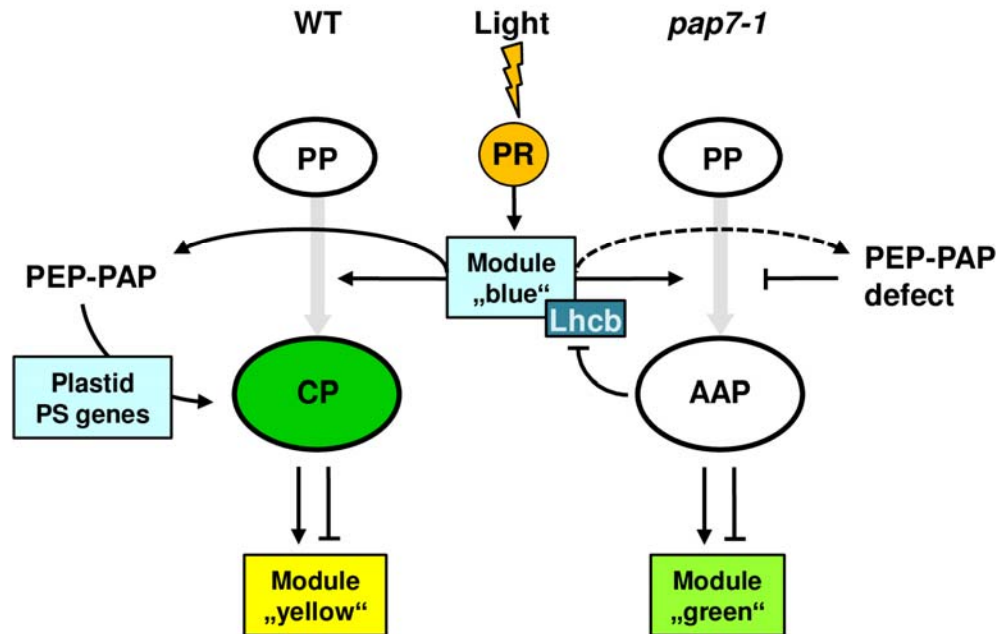


**Figure 8.** Model of anterograde and retrograde signalling during early steps of chloroplast biogenesis in Wt and *pap7-1* mutants. Light signals (flash) are perceived by photoreceptors (PR) (orange circle). Small white ovals represent undifferentiated pro-/eoplasts present in seeds. Large ovals in green and white represent the different plastid types in WT (CP) and *pap7-1* (AAP) seedlings. Grey bold arrows indicate the developmental process leading to these plastid types. Boxes indicate and name the genes or gene modules regulated during these processes. Thin black arrows represent positive regulation, lines with a blocking bar represent negative regulation.

551 repression by retrograde signals from the arrested plastid development. Only a few *Lhcb*  
 552 genes appeared to be selectively targeted by plastid signals (Fig. 5) and these, in addition,  
 553 seem to interact with light (Figs. 3, 5). This may explain the manifold connections identified  
 554 between light and plastid signaling using promoters of these genes in genetic screens and  
 555 corresponding mutants (Larkin, 2014). Interestingly, the structural and functional defect in the  
 556 PEP-PAP complex in *pap7-1* mutants does not affect the transcript accumulation of other  
 557 nuclear encoded components of the plastid transcription machinery (Fig. 5B) implying that  
 558 these genes are not under retrograde control.

559 It remains to understand why chloroplast biogenesis does not work in the mutant. A major  
 560 determinant of this developmental block certainly is the reduced expression of plastid  
 561 photosystem II genes, but the finding of residual transcripts suggests that likely also other  
 562 molecular reasons play a role such as the obvious inhibition of Chl biosynthesis (Gao et al.,  
 563 2012) as well as further defects that are unknown to date. We conclude that in the *pap7-1*  
 564 mutant especially plastidial photosystem II genes are strongly repressed while retrograde

565 signals from the arrested albino plastid neither modulate nor antagonistically counteract light  
566 regulation of PhANGs. This is different from conclusions obtained in recent studies on  
567 retrograde signaling using lincomycin, an inhibitor of plastid translation (Ruckle et al., 2007;  
568 Martin et al., 2016). Since *pap7-1* mutants developed rather normal in the first few days even  
569 without sugar we regard it as likely that either the genetic block in *pap7-1* mutants results in  
570 milder effects than a lincomycin treatment or the observed differences are due to technical  
571 differences in the respective set-ups, e.g. light intensity. Both scenarios suggest that there  
572 exists a threshold for the effectiveness of retrograde signals. Elucidating the molecular  
573 nature for this will be an interesting topic for future research. The retrograde-controlled gene  
574 groups identified in this study provide a useful first tool for such investigations.

575 An interesting result of our expression profiling was the identification of separate biogenic  
576 signals from chloroplasts and albino plastids. Chloroplast signal-dependent GO groups were  
577 mostly related to metabolism, likely because chloroplast biogenesis initiates the conversion  
578 from a heterotrophic to autotrophic life style. This includes the down-regulation of beta-  
579 oxidation of fatty acids that takes place in glyoxisomes. Oppositely GO groups for  
580 glucosinolate biosynthesis and indoleacetic acid biosynthesis were activated, both being  
581 highly important for pathogen defense and growth of green plants (Fig.7 B). GO groups  
582 regulated by signals from the arrested albino plastid relate mostly to starvation processes  
583 and the mobilization of storage energies (nitrogen compound metabolic processes,  
584 reproductive system development) being indicative of the non-autotrophic metabolism in the  
585 albino plantlets that requires the mobilization of all internal resources. Surprisingly a  
586 significant impact on the GO group of circadian rhythm was observed that suggests an  
587 influence of the plastid developmental stage on circadian clock genes. A circadian control  
588 from the nucleus influencing chloroplast transcription has been recently reported (Noordally  
589 et al., 2013). Furthermore, iron metabolism and plastid developmental stage were  
590 demonstrated to have a significant influence on the period of the circadian clock (Salome et  
591 al., 2013). These observations suggest that our results reflect a mutual influence between  
592 plastids and the circadian clock of larger significance providing an interesting target for future  
593 research (Fig. 7C).

594 In sum, the arrest of chloroplast development in the *pap7-1* mutant can be best explained by  
595 a specific disturbance in the light-induced build-up of the PEP complex during the pro-  
596 /eoplast-to-chloroplast transition. This leads to concomitant defects in the expression of PSII  
597 components and tRNAs, which in turn limits Chl biosynthesis and (likely) translation. The  
598 albinism of the mutant, thus, likely is the result of a multi-factorial syndrome that prevents  
599 chloroplast biogenesis without destroying the plastid. Therefore, the functional and metabolic  
600 state of the arrested albino plastid resembles that of an etioplast despite it is perceiving light.

601 This likely allows the mutant to develop normally when the lack of photosynthesis is  
602 complemented by an external carbon source. Correspondingly the overall gene expression  
603 profiles of *pap7-1* mutants do exhibit a chimerical character with metabolic genes regulated  
604 like in dark-grown seedlings and photo-regulated genes like in light-grown plants. In sum, the  
605 *pap7-1* mutant, but likely also other *pap* mutants provide an interesting tool for dissecting  
606 further the molecular processes during the early steps in chloroplast biogenesis.

607

## 608 **MATERIALS AND METHODS**

### 609 **Plant material**

610 We used *Arabidopsis thaliana* Columbia (Col) 0 as WT throughout the study. As null alleles  
611 for the genes *pap7-1/ptac14* and *pap6/fln1* we used the *Arabidopsis* T-DNA inactivation lines  
612 SAIL\_566\_F06 and GK-443A08, respectively. These lines (named *pap7-1* and *pap6-1* in this  
613 study) were characterized earlier in detail for singularity of T-DNA insertion and for causal  
614 connection between the albino phenotype and the corresponding gene defect (Arsova et al.,  
615 2010; Gao et al., 2011; Steiner et al., 2011; Gilkerson et al., 2012). Seeds of WT and  
616 heterozygous mutants were surface-sterilized and spread on half-strength standard MS  
617 medium supplemented with indicated amounts of sucrose in Petri dishes, stratified for 3 days  
618 and grown to the two-cotyledon stage at 21°C for further analyses. Light-grown plants used  
619 for array analyses were grown under permanent white light of 120-150  $\mu\text{E}$  photon flux  
620 density. In long-term growth experiments the illumination intensity of the white light source  
621 was reduced to 8-12  $\mu\text{E}$ .

### 622 **Plastid macro-array analysis**

623 Plant material was grown 6 days on MS medium supplemented with 0.5% sucrose. Around  
624 500 mg each of green WT and albino mutant cotyledons were harvested separately and  
625 shock-frozen in liquid nitrogen. Total RNA was isolated following published procedures  
626 (Demarsy et al., 2006; Demarsy et al., 2012). Potential DNA contaminations were removed  
627 by DNase treatment and its absence was proven by PCR. For preparation of the  
628 hybridization probe 4  $\mu\text{g}$  of each RNA preparation were reverse-transcribed using a gene-  
629 specific primer mix annealing to 80 protein-coding genes and their corresponding antisense  
630 sequences. Subsequently, a reverse transcription reaction was performed using Superscript  
631 II Reverse Transcriptase in presence of all four nucleotides and 100  $\mu\text{Ci}$  [ $\alpha$ - $^{32}\text{P}$ ] dATP  
632 (Demarsy et al., 2012). Unincorporated nucleotides were finally removed from the labelled  
633 cDNAs by gel-filtration through a Sephadex G50 column. For evaluation of relative  
634 differences in plastid transcription between the biological backgrounds of the two samples we

635 measured the total radioactivity of each cDNA sample after synthesis and verified the cDNA  
636 profile on a sequencing gel. In the experiment described here radioactively labelled cDNAs of  
637 WT and *pap7-1* differed by just 3% (WT>*pap7-1*) in incorporation indicating that total plastid  
638 gene expression is not significantly different in WT and *pap7-1* plantlets. Subsequent  
639 hybridization of the radiolabelled probes with the macroarray, washing conditions,  
640 subsequent signal detection in a phosphorimager (Fujifilm FLA-8000) and final data analysis  
641 were done essentially as described (Demarsy et al., 2012). Construction of the plastome  
642 macroarray including description of the gene-specific sense and antisense probes as well as  
643 their spotting pattern were published elsewhere (Lerbs-Mache, 2011).

#### 644 **Genome-wide micro-array analysis**

645 Plant material was grown on medium supplemented with 1% sugar in order harmonize the  
646 germination. Illuminated WT and homozygous *pap7-1* mutants were grown for 5 days for full  
647 expansion of the cotyledons while dark-grown WT seedlings were grown for 4 days in order  
648 to avoid mechanical stress imposed by physical contact with the lid of the Petri dishes. Plant  
649 materials were harvested 10:00 in the morning and shock frozen in liquid nitrogen. Dark  
650 grown material was harvested and shock-frozen at the same time point of the day, but under  
651 a green safe-light in order to exclude any light effects in the profiles. Total RNA from these  
652 materials then was basically prepared as described (Logemann et al., 1987). In brief, 250 mg  
653 of frozen plant material was ground in a mortar and purified with the Qiagen RNeasy  
654 purification kit. Concentration and purity of RNA samples were determined spectroscopically  
655 and intactness was proven by ethidium bromide staining after separation on 1.2% agarose  
656 gels. Purified samples from three biological replicates each were sent on dry ice to a  
657 commercial service (Kompetenzzentrum für Fluoreszenz Bioanalytik (KFB) Regensburg,  
658 Germany) where a second quality check, cDNA synthesis and labelling was performed  
659 according to the GeneChip 3' IVT Express Kit protocol (Affymetrix). Hybridisation and reading  
660 of signals were performed using the Arabidopsis Genome Array ATH1 (Affymetrix, USA) and  
661 according to standard protocols of the service.

662

#### 663 **Quantitative reverse transcription PCR analysis (qRT-PCR)**

664 Reverse transcription was performed with 1 µg total RNA isolated from three independent  
665 biological replicates of WT, *pap7-1* and *pap6* mutants grown identically as for the microarray  
666 analyses. cDNA was synthesized using oligo(dT) primers and the Invitrogen™ SuperScript™  
667 II Reverse Transcriptase following the manufacturers' recommendations. qRT-PCR was  
668 performed using the GoTaq® qPCR Master Mix (Promega) and the Rotor-Gene 3000™  
669 equipment. Primer sequences for genes of interest were designed using ApE-A plasmid  
670 Editor (v2.0.47) and NCBI/ Primer-BLAST (Basic Local Alignment Search Tool) with

671 preference to intron spanning amplicons. Each primer pair was tested for amplification  
672 efficiency using the synthesized cDNA. Only primer pairs with amplification efficiencies  
673 between 90% and 110% were used for further analysis. For used primer sequences and  
674 gene identities see Supplemental Table 4. The relative quantification was calculated  
675 according to described methods (Pfaffl, 2001). The *Arabidopsis* genes for actin 7 and  
676 ubiquitin 5 were used as internal control and reference genes for quantification.

677

## 678 **Bioinformatics**

679 In the supervised analysis the hybridization signal data from the microarray analysis  
680 performed by a commercial service (KFB Regensburg, Germany) were analyzed with the  
681 ROBINA (<http://mapman.gabipd.org/web/guest/robin-download>) and MapMan  
682 (<http://mapman.gabipd.org/web/guest/robin-download>) programmes (Usadel et al., 2005;  
683 Usadel et al., 2009). Statistical analysis by t-test and subsequent calculation of the false  
684 discovery rate were performed according to the ROBINA programme. Gene expression  
685 changes with a FDR of  $p \leq 0.05$  were regarded as statistically significant. The microarray  
686 data given in the Supplemental file 1 are based on three biological replicates each. The data  
687 discussed in this publication have been deposited in NCBI's Gene Expression Omnibus  
688 (Edgar et al., 2002; Barrett et al., 2013) and are accessible through GEO Series accession  
689 number GSE88988 (<https://www.ncbi.nlm.nih.gov/geo/query/acc.cgi?acc=GSE88988>).  
690 Visualization of the cellular pathways and functional categories of the expression data was  
691 carried out using the MapMan and Pegman package according to  
692 Ath\_AFFY\_ATH1\_TAIR8\_Jan 2010 (<http://mapman.gabipd.org>) (Usadel et al., 2005). The  
693 visualization tool of MapMan was used to identify similarities and differences in the different  
694 metabolic pathways. A Wilcoxon rank sum test was used to visualize significantly expressed  
695 genes in Pegman (Usadel et al., 2009). Venn diagrams were calculated using the expression  
696 log values of Map-man package. In the un-supervised WGCNA the original CEL files  
697 supplied by the commercial service were imported into R with Bioconductor (package oligo)  
698 (Carvalho and Irizarry, 2010) followed by normalization and background correction of the raw  
699 data using RMA. After selecting 27296 annotated genes a scaling and centering followed by  
700 a cluster analysis was performed. Differentially expressed genes were then selected with  
701 ANOVA and a FDR threshold of 0.05 followed by a WGCNA (Langfelder and Horvath, 2008)  
702 and a GO enrichment analysis using the R package topGO (Alexa and Rahnenführer,  
703 <http://www.mpi-sb.mpg.de/~alexa>).

704

## 705 **SUPPLEMENTAL MATERIALS**

706 **Supplemental Figure 1.** Relative gene expression profiles of WT and *pap7-1* mutants  
707 visualized using the MapMan tool.

708 **Supplemental Figure 2:** Correlation of expression data from selected genes obtained from  
709 microarrays and qRT-PCR.

710 **Supplemental Figure 3:** Identification of gene modules responsive to light and/or biogenic  
711 plastid signals with a significance threshold of  $\log_2 fc \geq 1$ .

712 **Supplemental Figure 4:** Weighted gene co-expression network cluster analysis.

713 **Supplemental Figure 5:** Gene ontology groups within module “Blue”.

714 **Supplemental Figure 6:** Gene ontology groups within module “Yellow”.

715 **Supplemental Figure 7:** Gene ontology groups within module “Green”.

716 **Supplemental Table 1:** Gene expression changes of genes sorted according to the  
717 encoding genomic compartment.

718 **Supplemental Table 2:** Gene sets with an expression change larger than the threshold 2  
719 [ $\log_2$ ].

720 **Supplemental Table 3:** Gene sets with an expression change larger than the threshold 1  
721 [ $\log_2$ ].

722 **Supplemental Table 4:** Nucleotide sequences of primers used for qRT-PCR.

723 **Supplemental Datasets 1-3**

724

725

## 726 **FIGURE LEGENDS**

727 **Figure 1.** Developmental characteristics of the *pap7-1* mutant. A, 72h-dark-grown progeny of  
728 a *pap7-1/+* heterozygote subjected to 24h of 20  $\mu$ E white light to trigger  
729 photomorphogenesis. White arrowheads indicate a *pap7-1* homozygote mutant before and  
730 after subjection to light. Hypocotyl length +/- standard deviation measured after 72 h of dark  
731 growth. Genotypes were assigned after 24 h of light exposure (n= number of  
732 measurements). B, Growth of homozygous *pap7-1* seedlings and WT on  $\frac{1}{2}$  strength MS-  
733 medium in Petri-dishes without or with (+ suc) sucrose supplementation. C, Impact of *pap7-1*  
734 inactivation on chloroplast development during transient embryo greening and seed

735 segregation in siliques of heterozygous *pap7-1* mutants (*pap7-1/+*) in comparison to WT (two  
736 left panels). Long-term growth (8 weeks) of the progeny of heterozygous mutants was  
737 performed on ½ strength MS-medium supplemented with 3% sucrose in transparent plastic  
738 containers in a short-day light period (right panel). Seed segregation into green and  
739 colourless seeds was counted in 7-10 siliques per measurement day (7 or 9 days after  
740 fertilization) in WT and *pap7-1/+* mutants (bottom panel). D, Long-term grown plants in  
741 rosette stage were put into long-day conditions to induce flowering and photographed at the  
742 flowering stage.

743

744 **Figure 2.** Macro-array analysis comparing plastid transcript accumulation in light-grown wild-  
745 type and *pap7-1 Arabidopsis* seedlings. Given is the transcript accumulation in wild-type (top  
746 panel) and mutant (bottom panel) seedlings both for sense (blue bars) and anti-sense (red  
747 bars) transcripts. Hybridization signals were normalized to the total signal intensity of the  
748 membrane and are given as arbitrary units in the left margin. Genes are labeled at the  
749 bottom of each panel according to accepted nomenclatures. Sequence of genes corresponds  
750 to their organization on the plastome separated between inner strand (left parts) and outer  
751 strand of the plastome (right parts). High transcript accumulation of PEP-dependent  
752 transcripts in WT is high-lighted by green boxes. High transcript accumulation of NEP-  
753 dependent transcripts in the *pap7-1* mutant is high-lighted by yellow boxes.

754 **Figure 3.** Identification of gene modules responsive to light and/or biogenic plastid signals.  
755 A, Strategy for differential expression profiling of 4-5-day-old *Arabidopsis* seedlings in  
756 wildtype (WT) and *pap7-1* mutants (*pap7-1*). Left panel displays photographs of seedlings  
757 with representative phenotypic appearance. The right panel indicates the corresponding  
758 developmental transition of the plastids in each of these seedlings. White small ovals  
759 represent undifferentiated pro-/eoplasts from seeds. Upon illumination they develop into  
760 green chloroplasts (CP) in WT (WT light) or arrested albino plastids (AAP) in *pap7* mutants  
761 (*pap7-1* light). Growth in the dark leads to development of yellow etioplasts (ET) in WT (WT  
762 dark). Analysis of differences between expression profiles in these plant samples (indicated  
763 by brackets) identify genes for photomorphogenesis (PM), for plastid-independent light  
764 signaling (LS) and for plastid signalling (PS) (for details see text). B, Flow diagramme of  
765 bioinformatic analysis done with primary expression data from the microarray analysis. C,  
766 Detailed comparison of differentially expressed genes (indicated by numbers) within the PM  
767 and LS expression modules according to their direction of expression change (indicated by  
768 arrows). Only genes exceeding a threshold of  $\log_2 \text{fc} \geq 2$  were taken into analysis. Genes  
769 found in both modules were further separated according to their direction and degree of gene  
770 expression change. Arrows of different size but same direction indicate genes that display

771 the same direction of expression change but with a difference of at least  $\log_2 \text{fc} \geq 1$ . Green  
772 arrows: Expression change in WT. White arrows: Expression change in *pap7-1* mutants. For  
773 more details see legend box. D, Proportional distribution of genes within the different gene  
774 groups defined in Fig. 3C according to their functional association within MapMan bins.

775 **Figure 4.** Expression profiles of selected genes from the microarray analysis tested by qRT-  
776 PCR. A, Expression changes of genes representative for distinct expression classes in WT-  
777 light, *pap7-1* and *pap6-1* mutants compared to WT-dark. Genes for proteins Lhcb1.4,  
778 Lhcb1.2 and oePEL (light harvesting complex II proteins 1.4 and 1.2, “overexpression leads  
779 to pseudo-etiolation in light”) represent genes displaying a reduced light induction in *pap7-1*  
780 when compared to WT. Genes encoding proteins STN7, PGRL1a and SIG5 (state transition  
781 kinase 7, PGR5-like protein 1a, sigma factor 5) represent genes displaying no effect of *pap7-1*  
782 on light induction, while the gene for PORB (protochlorophyllide oxidoreductase B)  
783 represents an example for strong light repression both in WT and *pap7-1* mutant. The genes  
784 for ATGPX7 and UVR3 (glutathione peroxidase 7 and (6-4) DNA photolyase) were used as  
785 examples displaying light induction in WT and further promotion in *pap7-1*. Genes for SEN1  
786 and HFR1 (senescence-associated protein DIN1 and the transcription factor Long Hypocotyl  
787 after far-red 1) represent genes displaying repression in WT but promotion in the mutant. As  
788 additional genetic control *pap6-1/fln1* (defective in the gene for a phospho-fructokinase like 1  
789 protein) was used in order to detect potential mutation-specific responses. Expression of  
790 both *pap* genes was tested in all RNA samples as further control. B, Difference in expression  
791 change between light grown WT and the *pap7-1* and *pap6-1* mutants. Negative values  
792 indicate lower expression, positive values higher expression than in WT. Data given  
793 represent means of three independent experiments. Primers used are given in Supplemental  
794 Table 4.

795 **Figure 5.** Light-induced expression changes of genes for photosynthesis and plastid  
796 transcription. A, The graphs display the expression values of significantly light-affected  
797 photosynthesis genes ( $\log_2 \geq 1$ ) detected by comparison of expression profiles WT-light  
798 versus WT-dark (top graph) and *pap7-1*-light versus WT-dark (bottom graph). From the 169  
799 photosynthesis genes present in the corresponding MapMan bin 72 and 62 genes,  
800 respectively, exhibited an expression change of at least  $\log_2 \geq 1$ . In the WT-light versus WT-  
801 dark comparison all plastid genes remained below this threshold. Genes exceeding an  
802 expression change of  $\log_2 \geq 2$  were boxed in the graph and listed in a panel aside. Nuclear  
803 encoded genes are given in black, plastid encoded genes are given in green. The difference  
804 in the expression change of a particular gene that occurs between the top and the bottom  
805 panel reflects the plastid influence on its expression. Strongly down-regulated genes in *pap7-1*-  
806 light versus WT-dark ( $\log_2 \geq -1$ ) are given in a left box. B, Expression changes for all 31



807 nuclear genes encoding components of the plastid gene transcription machinery in WT and  
808 *pap7-1*. The respective comparisons are indicated in the top panel, gene identities in the left  
809 and protein identities in the right panels. Given values represent log 2 fold changes, a  
810 corresponding color code is depicted at the bottom level.

811 **Figure 6.** Cluster analysis of genes differentially regulated in the three growth set-ups as  
812 defined by ANOVA. Genes displaying a FDR of < 0.05 were included. The right margin  
813 identified the data sets from the microarray analysis, the left margin indicates a cladogramme  
814 defining the correlation in gene expression profiles between them. On top clustering of gene  
815 groups according to their expression is indicated. Diagramme in top left corner gives the  
816 color key and numbers of genes with corresponding gene expression values. Red: Up-  
817 regulation. Green: Down-regulation.

818 **Figure 7.** GO groups of differentially expressed gene sets within the gene modules identified  
819 by WGCNA. A, Gene module „blue“ with four major gene groups regulated by light. B, Gene  
820 module „yellow“ with six major gene groups regulated by the chloroplast. C, Gene module  
821 „green“ with three major gene groups specifically regulated by the arrested plastid. Genes  
822 displaying a FDR of < 0.05 were included. On top of each heat map the selected GO group is  
823 given, underneath a clustering of the genes in this group according to their expression is  
824 indicated. The right margin identifies the data sets from the microarray analysis. Red: Up-  
825 regulation. Green: Down-regulation. For further gene groups see Supplemental Files 8-10.

826

827 **Figure 8.** Model of anterograde and retrograde signalling during early steps of chloroplast  
828 biogenesis in Wt and *pap7-1* mutants. Light signals (flash) are perceived by photoreceptors  
829 (PR) (orange circle). Small white ovals represent undifferentiated pro-/eoplasts present in  
830 seeds. Large ovals in green and white represent the different plastid types in WT (CP) and  
831 *pap7-1* (AAP) seedlings. Grey bold arrows indicate the developmental process leading to  
832 these plastid types. Boxes indicate and name the genes or gene modules regulated during  
833 these processes. Thin black arrows represent positive regulation, lines with a blocking bar  
834 represent negative regulation.

835

836

## Parsed Citations

**Allorent G, Courtois F, Chevalier F, Lerbs-Mache S (2013) Plastid gene expression during chloroplast differentiation and dedifferentiation into non-photosynthetic plastids during seed formation. *Plant Mol Biol* 82: 59-70**

Pubmed: [Author and Title](#)

CrossRef: [Author and Title](#)

Google Scholar: [Author Only](#) [Title Only](#) [Author and Title](#)

**Arsova B, Hoja U, Wimmelbacher M, Greiner E, Ustun S, Melzer M, Petersen K, Lein W, Bornke F (2010) Plastidial thioredoxin z interacts with two fructokinase-like proteins in a thiol-dependent manner: evidence for an essential role in chloroplast development in *Arabidopsis* and *Nicotiana benthamiana*. *Plant Cell* 22: 1498-1515**

Pubmed: [Author and Title](#)

CrossRef: [Author and Title](#)

Google Scholar: [Author Only](#) [Title Only](#) [Author and Title](#)

**Arsovski AA, Galstyan A, Guseman JM, Nemhauser JL (2012) Photomorphogenesis. *Arabidopsis Book* 10: e0147**

Pubmed: [Author and Title](#)

CrossRef: [Author and Title](#)

Google Scholar: [Author Only](#) [Title Only](#) [Author and Title](#)

**Barrett T, Wilhite SE, Ledoux P, Evangelista C, Kim IF, Tomashevsky M, Marshall KA, Phillippy KH, Sherman PM, Holko M, Yefanov A, Lee H, Zhang N, Robertson CL, Serova N, Davis S, Soboleva A (2013) NCBI GEO: archive for functional genomics data sets--update. *Nucleic Acids Res* 41 (Database issue): D991-995**

Pubmed: [Author and Title](#)

CrossRef: [Author and Title](#)

Google Scholar: [Author Only](#) [Title Only](#) [Author and Title](#)

**Borner T, Aleynikova AY, Zubo YO, Kusnetsov VV (2015) Chloroplast RNA polymerases: Role in chloroplast biogenesis. *Biochim Biophys Acta* 1847: 761-769**

Pubmed: [Author and Title](#)

CrossRef: [Author and Title](#)

Google Scholar: [Author Only](#) [Title Only](#) [Author and Title](#)

**Brown NJ, Sullivan JA, Gray JC (2005) Light and plastid signals regulate the expression of the pea plastocyanin gene through a common region at the 5' end of the coding region. *Plant J* 43: 541-552**

Pubmed: [Author and Title](#)

CrossRef: [Author and Title](#)

Google Scholar: [Author Only](#) [Title Only](#) [Author and Title](#)

**Carvalho BS, Irizarry RA (2010) A Framework for Oligonucleotide Microarray Preprocessing. *Bioinformatics* 26: 2363-2367**

Pubmed: [Author and Title](#)

CrossRef: [Author and Title](#)

Google Scholar: [Author Only](#) [Title Only](#) [Author and Title](#)

**Chan KX, Phua SY, Crisp P, McQuinn R, Pogson BJ (2016) Learning the Languages of the Chloroplast: Retrograde Signaling and Beyond. *Annu Rev Plant Biol* 67: 25-53**

Pubmed: [Author and Title](#)

CrossRef: [Author and Title](#)

Google Scholar: [Author Only](#) [Title Only](#) [Author and Title](#)

**Chi W, Sun X, Zhang L (2013) Intracellular signaling from plastid to nucleus. *Annu Rev Plant Biol* 64: 559-582**

Pubmed: [Author and Title](#)

CrossRef: [Author and Title](#)

Google Scholar: [Author Only](#) [Title Only](#) [Author and Title](#)

**De Santis-Maclossek G, Kofer W, Bock A, Schoch S, Maier RM, Wanner G, Rudiger W, Koop HU, Herrmann RG (1999) Targeted disruption of the plastid RNA polymerase genes rpoA, B and C1: molecular biology, biochemistry and ultrastructure. *Plant J* 18: 477-489**

Pubmed: [Author and Title](#)

CrossRef: [Author and Title](#)

Google Scholar: [Author Only](#) [Title Only](#) [Author and Title](#)

**de Souza A, Wang JZ, Dehesh K (2016) Retrograde Signals: Integrators of Interorganellar Communication and Orchestrators of Plant Development. *Annu Rev Plant Biol***

Pubmed: [Author and Title](#)

CrossRef: [Author and Title](#)

Google Scholar: [Author Only](#) [Title Only](#) [Author and Title](#)

**Demarsy E, Buhr F, Lambert E, Lerbs-Mache S (2012) Characterization of the plastid-specific germination and seedling establishment transcriptional programme. *J Exp Bot* 63: 925-939**

Pubmed: [Author and Title](#)

CrossRef: [Author and Title](#)

Google Scholar: [Author Only](#) [Title Only](#) [Author and Title](#)

**Demarsy E, Courtois F, Azevedo J, Buhot L, Lerbs-Mache S (2006) Building up of the plastid transcriptional machinery during**

Downloaded from on September 28, 2017 - Published by www.plantphysiol.org

Copyright © 2017 American Society of Plant Biologists. All rights reserved.

germination and early plant development. *Plant Physiol* 142: 993-1003

Pubmed: [Author and Title](#)

CrossRef: [Author and Title](#)

Google Scholar: [Author Only Title Only Author and Title](#)

Edgar R, Domrachev M, Lash AE (2002) Gene Expression Omnibus: NCBI gene expression and hybridization array data repository. *Nucleic Acids Res* 30: 207-210

Pubmed: [Author and Title](#)

CrossRef: [Author and Title](#)

Google Scholar: [Author Only Title Only Author and Title](#)

Eisermann A, Tiller K, Link G (1990) In vitro transcription and DNA binding characteristics of chloroplast and etioplast extracts from mustard (*Sinapis alba*) indicate differential usage of the psbA promoter. *EMBO J* 9: 3981-3987

Pubmed: [Author and Title](#)

CrossRef: [Author and Title](#)

Google Scholar: [Author Only Title Only Author and Title](#)

Estavillo GM, Crisp PA, Pornsiriwong W, Wirtz M, Collinge D, Carrie C, Giraud E, Whelan J, David P, Javot H, Brearley C, Hell R, Marin E, Pogson BJ (2011) Evidence for a SAL1-PAP chloroplast retrograde pathway that functions in drought and high light signaling in *Arabidopsis*. *Plant Cell* 23: 3992-4012

Pubmed: [Author and Title](#)

CrossRef: [Author and Title](#)

Google Scholar: [Author Only Title Only Author and Title](#)

Galvez-Valdivieso G, Fryer MJ, Lawson T, Slattery K, Truman W, Smirnoff N, Asami T, Davies WJ, Jones AM, Baker NR, Mullineaux PM (2009) The high light response in *Arabidopsis* involves ABA signaling between vascular and bundle sheath cells. *Plant Cell* 21: 2143-2162

Pubmed: [Author and Title](#)

CrossRef: [Author and Title](#)

Google Scholar: [Author Only Title Only Author and Title](#)

Gao ZP, Chen GX, Yang ZN (2012) Regulatory role of *Arabidopsis* pTAC14 in chloroplast development and plastid gene expression. *Plant Signal Behav* 7: 1354-1356

Pubmed: [Author and Title](#)

CrossRef: [Author and Title](#)

Google Scholar: [Author Only Title Only Author and Title](#)

Gao ZP, Yu QB, Zhao TT, Ma Q, Chen GX, Yang ZN (2011) A functional component of the transcriptionally active chromosome complex, *Arabidopsis* pTAC14, interacts with pTAC12/HEMERA and regulates plastid gene expression. *Plant Physiol* 157: 1733-1745

Pubmed: [Author and Title](#)

CrossRef: [Author and Title](#)

Google Scholar: [Author Only Title Only Author and Title](#)

Gilkerson J, Perez-Ruiz JM, Chory J, Callis J (2012) The plastid-localized pfkB-type carbohydrate kinases FRUCTOKINASE-LIKE 1 and 2 are essential for growth and development of *Arabidopsis thaliana*. *BMC Plant Biol* 12: 102

Pubmed: [Author and Title](#)

CrossRef: [Author and Title](#)

Google Scholar: [Author Only Title Only Author and Title](#)

Hajdukiewicz PT, Allison LA, Maliga P (1997) The two RNA polymerases encoded by the nuclear and the plastid compartments transcribe distinct groups of genes in tobacco plastids. *EMBO J* 16: 4041-4048

Pubmed: [Author and Title](#)

CrossRef: [Author and Title](#)

Google Scholar: [Author Only Title Only Author and Title](#)

Hills AC, Khan S, Lopez-Juez E (2015) Chloroplast Biogenesis-Associated Nuclear Genes: Control by Plastid Signals Evolved Prior to Their Regulation as Part of Photomorphogenesis. *Front Plant Sci* 6: 1078

Pubmed: [Author and Title](#)

CrossRef: [Author and Title](#)

Google Scholar: [Author Only Title Only Author and Title](#)

Isemer R, Mulisch M, Schafer A, Kirchner S, Koop HU, Krupinska K (2012) Recombinant Whirly1 translocates from transplastomic chloroplasts to the nucleus. *FEBS Lett* 586: 85-88

Pubmed: [Author and Title](#)

CrossRef: [Author and Title](#)

Google Scholar: [Author Only Title Only Author and Title](#)

Kleine T, Leister D (2016) Retrograde signaling: Organelles go networking. *Biochim Biophys Acta* 1857: 1313-1325

Pubmed: [Author and Title](#)

CrossRef: [Author and Title](#)

Google Scholar: [Author Only Title Only Author and Title](#)

Klie S, Nikoloski Z (2012) The Choice between MapMan and Gene Ontology for Automated Gene Function Prediction in Plant Science. *Front Genet* 3: 115

Pubmed: [Author and Title](#)

CrossRef: [Author and Title](#)  
Google Scholar: [Author Only Title Only Author and Title](#)

**Kusnetsov V, Bolle C, Lubberstedt T, Sopory S, Herrmann RG, Oelmuller R (1996) Evidence that the plastid signal and light operate via the same cis-acting elements in the promoters of nuclear genes for plastid proteins. Mol Gen Genet 252: 631-639**

Pubmed: [Author and Title](#)  
CrossRef: [Author and Title](#)  
Google Scholar: [Author Only Title Only Author and Title](#)

**Lagrange T, Hakimi MA, Pontier D, Courtois F, Alcaraz JP, Grunwald D, Lam E, Lerbs-Mache S (2003) Transcription factor IIB (TFIIB)-related protein (pBrp), a plant-specific member of the TFIIB-related protein family. Mol Cell Biol 23: 3274-3286**

Pubmed: [Author and Title](#)  
CrossRef: [Author and Title](#)  
Google Scholar: [Author Only Title Only Author and Title](#)

**Langfelder P, Horvath S (2008) WGCNA: an R package for weighted correlation network analysis. BMC Bioinformatics 9: 559**

Pubmed: [Author and Title](#)  
CrossRef: [Author and Title](#)  
Google Scholar: [Author Only Title Only Author and Title](#)

**Larkin RM (2014) Influence of plastids on light signalling and development. Philos Trans R Soc Lond B Biol Sci 369: 20130232**

Pubmed: [Author and Title](#)  
CrossRef: [Author and Title](#)  
Google Scholar: [Author Only Title Only Author and Title](#)

**Lee KP, Kim C, Landgraf F, Apel K (2007) EXECUTER1- and EXECUTER2-dependent transfer of stress-related signals from the plastid to the nucleus of Arabidopsis thaliana. Proc Natl Acad Sci U S A 104: 10270-10275**

Pubmed: [Author and Title](#)  
CrossRef: [Author and Title](#)  
Google Scholar: [Author Only Title Only Author and Title](#)

**Legen J, Kemp S, Krause K, Profanter B, Herrmann RG, Maier RM (2002) Comparative analysis of plastid transcription profiles of entire plastid chromosomes from tobacco attributed to wild-type and PEP-deficient transcription machineries. Plant J 31: 171-188**

Pubmed: [Author and Title](#)  
CrossRef: [Author and Title](#)  
Google Scholar: [Author Only Title Only Author and Title](#)

**Lerbs-Mache S (2011) Function of plastid sigma factors in higher plants: regulation of plastid gene expression or just preservation of constitutive transcription? Plant Mol Biol 76: 235-249**

Pubmed: [Author and Title](#)  
CrossRef: [Author and Title](#)  
Google Scholar: [Author Only Title Only Author and Title](#)

**Liebers M, Grubler B, Chevalier F, Lerbs-Mache S, Merendino L, Blanvillain R, Pfannschmidt T (2017) Regulatory Shifts in Plastid Transcription Play a Key Role in Morphological Conversions of Plastids during Plant Development. Front Plant Sci 8: 23**

Pubmed: [Author and Title](#)  
CrossRef: [Author and Title](#)  
Google Scholar: [Author Only Title Only Author and Title](#)

**Liere K, Weihe A, Borner T (2011) The transcription machineries of plant mitochondria and chloroplasts: Composition, function, and regulation. J Plant Physiol 168: 1345-1360**

Pubmed: [Author and Title](#)  
CrossRef: [Author and Title](#)  
Google Scholar: [Author Only Title Only Author and Title](#)

**Logemann J, Schell J, Willmitzer L (1987) Improved method for the isolation of RNA from plant tissues. Analytical Biochemistry 163: 16-20**

Pubmed: [Author and Title](#)  
CrossRef: [Author and Title](#)  
Google Scholar: [Author Only Title Only Author and Title](#)

**Lopez-Juez E (2007) Plastid biogenesis, between light and shadows. J Exp Bot 58: 11-26**

Pubmed: [Author and Title](#)  
CrossRef: [Author and Title](#)  
Google Scholar: [Author Only Title Only Author and Title](#)

**Lopez-Juez E, Jarvis RP, Takeuchi A, Page AM, Chory J (1998) New Arabidopsis cue mutants suggest a close connection between plastid- and phytochrome regulation of nuclear gene expression. Plant Physiol 118: 803-815**

Pubmed: [Author and Title](#)  
CrossRef: [Author and Title](#)  
Google Scholar: [Author Only Title Only Author and Title](#)

**Ma L, Li J, Qu L, Hager J, Chen Z, Zhao H, Deng XW (2001) Light control of Arabidopsis development entails coordinated regulation of genome expression and cellular pathways. Plant Cell 13: 2589-2607**

Pubmed: [Author and Title](#)  
CrossRef: [Author and Title](#)

Google Scholar: [Author Only](#) [Title Only](#) [Author and Title](#)

**Martin G, Leivar P, Ludevid D, Tepperman JM, Quail PH, Monte E (2016) Phytochrome and retrograde signalling pathways converge to antagonistically regulate a light-induced transcriptional network. Nat Commun 7: 11431**

Pubmed: [Author and Title](#)

CrossRef: [Author and Title](#)

Google Scholar: [Author Only](#) [Title Only](#) [Author and Title](#)

**Noordally ZB, Ishii K, Atkins KA, Wetherill SJ, Kusakina J, Walton EJ, Kato M, Azuma M, Tanaka K, Hanaoka M, Dodd AN (2013) Circadian control of chloroplast transcription by a nuclear-encoded timing signal. Science 339: 1316-1319**

Pubmed: [Author and Title](#)

CrossRef: [Author and Title](#)

Google Scholar: [Author Only](#) [Title Only](#) [Author and Title](#)

**Page MT, Kacprzak SM, Mochizuki N, Okamoto H, Smith AG, Terry MJ (2017) Seedlings Lacking the PTM Protein Do Not Show a genomes uncoupled (gun) Mutant Phenotype. Plant Physiol 174: 21-26**

Pubmed: [Author and Title](#)

CrossRef: [Author and Title](#)

Google Scholar: [Author Only](#) [Title Only](#) [Author and Title](#)

**Page MT, McCormac AC, Smith AG, Terry MJ (2017) Singlet oxygen initiates a plastid signal controlling photosynthetic gene expression. New Phytol 213: 1168-1180**

Pubmed: [Author and Title](#)

CrossRef: [Author and Title](#)

Google Scholar: [Author Only](#) [Title Only](#) [Author and Title](#)

**Park SW, Li W, Viehhauser A, He B, Kim S, Nilsson AK, Andersson MX, Kittle JD, Ambavaram MM, Luan S, Esker AR, Tholl D, Cimini D, Ellerstrom M, Coaker G, Mitchell TK, Pereira A, Dietz KJ, Lawrence CB (2013) Cyclophilin 20-3 relays a 12-oxo-phytodienoic acid signal during stress responsive regulation of cellular redox homeostasis. Proc Natl Acad Sci U S A 110: 9559-9564**

Pubmed: [Author and Title](#)

CrossRef: [Author and Title](#)

Google Scholar: [Author Only](#) [Title Only](#) [Author and Title](#)

**Pfaffl MW (2001) A new mathematical model for relative quantification in real-time RT-PCR. Nucleic Acids Res 29: 45**

Pubmed: [Author and Title](#)

CrossRef: [Author and Title](#)

Google Scholar: [Author Only](#) [Title Only](#) [Author and Title](#)

**Pfalz J, Liere K, Kandlbinder A, Dietz KJ, Oelmüller R (2006) pTAC2, -6, and -12 are components of the transcriptionally active plastid chromosome that are required for plastid gene expression. Plant Cell 18: 176-197**

Pubmed: [Author and Title](#)

CrossRef: [Author and Title](#)

Google Scholar: [Author Only](#) [Title Only](#) [Author and Title](#)

**Pfalz J, Pfannschmidt T (2013) Essential nucleoid proteins in early chloroplast development. Trends Plant Sci 18: 186-194**

Pubmed: [Author and Title](#)

CrossRef: [Author and Title](#)

Google Scholar: [Author Only](#) [Title Only](#) [Author and Title](#)

**Pfannschmidt T (2010) Plastidial retrograde signalling—a true "plastid factor" or just metabolite signatures? Trends Plant Sci 15: 427-435**

Pubmed: [Author and Title](#)

CrossRef: [Author and Title](#)

Google Scholar: [Author Only](#) [Title Only](#) [Author and Title](#)

**Pfannschmidt T, Blanvillain R, Merendino L, Courtois F, Chevalier F, Liebers M, Grubler B, Hommel E, Lerbs-Mache S (2015) Plastid RNA polymerases: orchestration of enzymes with different evolutionary origins controls chloroplast biogenesis during the plant life cycle. J Exp Bot 66: 6957-6973**

Pubmed: [Author and Title](#)

CrossRef: [Author and Title](#)

Google Scholar: [Author Only](#) [Title Only](#) [Author and Title](#)

**Pfannschmidt T, Link G (1994) Separation of two classes of plastid DNA-dependent RNA polymerases that are differentially expressed in mustard (*Sinapis alba* L.) seedlings. Plant Mol Biol 25: 69-81**

Pubmed: [Author and Title](#)

CrossRef: [Author and Title](#)

Google Scholar: [Author Only](#) [Title Only](#) [Author and Title](#)

**Pfannschmidt T, Munne-Bosch S (2013) Plastidial signaling during the plant life cycle. . In B Biswal, K Krupinska, eds, Plastid development in leaves during growth and senescence. Springer, Dordrecht**

Pubmed: [Author and Title](#)

CrossRef: [Author and Title](#)

Google Scholar: [Author Only](#) [Title Only](#) [Author and Title](#)

**Pogson BJ, Ganguly D, Albrecht-Borth V (2015) Insights into chloroplast biogenesis and development. Biochim Biophys Acta 1847:**

Downloaded from on September 28, 2017 - Published by www.plantphysiol.org

Copyright © 2017 American Society of Plant Biologists. All rights reserved.

1017-1024

Pubmed: [Author and Title](#)  
CrossRef: [Author and Title](#)  
Google Scholar: [Author Only](#) [Title Only](#) [Author and Title](#)

**Pogson BJ, Woo NS, Forster B, Small ID (2008) Plastid signalling to the nucleus and beyond. Trends Plant Sci 13: 602-609**

Pubmed: [Author and Title](#)  
CrossRef: [Author and Title](#)  
Google Scholar: [Author Only](#) [Title Only](#) [Author and Title](#)

**Pulido P, Perello C, Rodriguez-Concepcion M (2012) New insights into plant isoprenoid metabolism. Mol Plant 5: 964-967**

Pubmed: [Author and Title](#)  
CrossRef: [Author and Title](#)  
Google Scholar: [Author Only](#) [Title Only](#) [Author and Title](#)

**Ramel F, Birtic S, Ginies C, Soubigou-Taconnat L, Triantaphylides C, Havaux M (2012) Carotenoid oxidation products are stress signals that mediate gene responses to singlet oxygen in plants. Proc Natl Acad Sci U S A 109: 5535-5540**

Pubmed: [Author and Title](#)  
CrossRef: [Author and Title](#)  
Google Scholar: [Author Only](#) [Title Only](#) [Author and Title](#)

**Ruckle ME, Burgoon LD, Lawrence LA, Sinkler CA, Larkin RM (2012) Plastids are major regulators of light signaling in Arabidopsis. Plant Physiol 159: 366-390**

Pubmed: [Author and Title](#)  
CrossRef: [Author and Title](#)  
Google Scholar: [Author Only](#) [Title Only](#) [Author and Title](#)

**Ruckle ME, DeMarco SM, Larkin RM (2007) Plastid signals remodel light signaling networks and are essential for efficient chloroplast biogenesis in Arabidopsis. Plant Cell 19: 3944-3960**

Pubmed: [Author and Title](#)  
CrossRef: [Author and Title](#)  
Google Scholar: [Author Only](#) [Title Only](#) [Author and Title](#)

**Salome PA, Oliva M, Weigel D, Kramer U (2013) Circadian clock adjustment to plant iron status depends on chloroplast and phytochrome function. EMBO J 32: 511-523**

Pubmed: [Author and Title](#)  
CrossRef: [Author and Title](#)  
Google Scholar: [Author Only](#) [Title Only](#) [Author and Title](#)

**Steiner S, Schroter Y, Pfalz J, Pfannschmidt T (2011) Identification of essential subunits in the plastid-encoded RNA polymerase complex reveals building blocks for proper plastid development. Plant Physiol 157: 1043-1055**

Pubmed: [Author and Title](#)  
CrossRef: [Author and Title](#)  
Google Scholar: [Author Only](#) [Title Only](#) [Author and Title](#)

**Su YS, Lagarias JC (2007) Light-independent phytochrome signaling mediated by dominant GAF domain tyrosine mutants of Arabidopsis phytochromes in transgenic plants. Plant Cell 19: 2124-2139**

Pubmed: [Author and Title](#)  
CrossRef: [Author and Title](#)  
Google Scholar: [Author Only](#) [Title Only](#) [Author and Title](#)

**Sullivan JA, Gray JC (2002) Multiple plastid signals regulate the expression of the pea plastocyanin gene in pea and transgenic tobacco plants. Plant J 32: 763-774**

Pubmed: [Author and Title](#)  
CrossRef: [Author and Title](#)  
Google Scholar: [Author Only](#) [Title Only](#) [Author and Title](#)

**Sun X, Feng P, Xu X, Guo H, Ma J, Chi W, Lin R, Lu C, Zhang L (2011) A chloroplast envelope-bound PHD transcription factor mediates chloroplast signals to the nucleus. Nat Commun 2: 477**

Pubmed: [Author and Title](#)  
CrossRef: [Author and Title](#)  
Google Scholar: [Author Only](#) [Title Only](#) [Author and Title](#)

**Terry MJ, Smith AG (2013) A model for tetrapyrrole synthesis as the primary mechanism for plastid-to-nucleus signaling during chloroplast biogenesis. Frontiers in Plant Sciences 4: 14**

Pubmed: [Author and Title](#)  
CrossRef: [Author and Title](#)  
Google Scholar: [Author Only](#) [Title Only](#) [Author and Title](#)

**Tiller K, Link G (1993) Sigma-like transcription factors from mustard (Sinapis alba L.) etioplast are similar in size to, but functionally distinct from, their chloroplast counterparts. Plant Mol Biol 21: 503-513**

Pubmed: [Author and Title](#)  
CrossRef: [Author and Title](#)  
Google Scholar: [Author Only](#) [Title Only](#) [Author and Title](#)

**Usadel B, Nagel A, Thimm O, Rediger H, Blaschinger OE, Palacios-Rojas N, Seibig J, Hammermann J, Piques MC, Steinhauser D, Scheible**

**WR, Gibon Y, Morcuende R, Weicht D, Meyer S, Stitt M (2005) Extension of the visualization tool MapMan to allow statistical analysis of arrays, display of corresponding genes, and comparison with known responses. Plant Physiol 138: 1195-1204**

Pubmed: [Author and Title](#)

CrossRef: [Author and Title](#)

Google Scholar: [Author Only](#) [Title Only](#) [Author and Title](#)

**Usadel B, Poree F, Nagel A, Lohse M, Czedik-Eysenberg A, Stitt M (2009) A guide to using MapMan to visualize and compare Omics data in plants: a case study in the crop species, Maize. Plant Cell Environ 32: 1211-1229**

Pubmed: [Author and Title](#)

CrossRef: [Author and Title](#)

Google Scholar: [Author Only](#) [Title Only](#) [Author and Title](#)

**Waters MT, Langdale JA (2009) The making of a chloroplast. EMBO J 28: 2861-2873**

Pubmed: [Author and Title](#)

CrossRef: [Author and Title](#)

Google Scholar: [Author Only](#) [Title Only](#) [Author and Title](#)

**Williams-Carrier R, Zoschke R, Belcher S, Pfalz J, Barkan A (2014) A major role for the plastid-encoded RNA polymerase complex in the expression of plastid transfer RNAs. Plant Physiol 164: 239-248**

Pubmed: [Author and Title](#)

CrossRef: [Author and Title](#)

Google Scholar: [Author Only](#) [Title Only](#) [Author and Title](#)

**Woodson JD, Perez-Ruiz JM, Chory J (2011) Heme synthesis by plastid ferrochelatase I regulates nuclear gene expression in plants. Curr Biol 21: 897-903**

Pubmed: [Author and Title](#)

CrossRef: [Author and Title](#)

Google Scholar: [Author Only](#) [Title Only](#) [Author and Title](#)

**Xiao Y, Savchenko T, Baidoo EE, Chehab WE, Hayden DM, Tolstikov V, Corwin JA, Kliebenstein DJ, Keasling JD, Dehesh K (2012) Retrograde signaling by the plastidial metabolite MEcPP regulates expression of nuclear stress-response genes. Cell 149: 1525-1535**

Pubmed: [Author and Title](#)

CrossRef: [Author and Title](#)

Google Scholar: [Author Only](#) [Title Only](#) [Author and Title](#)

**Zghidi-Abouzid O, Merendino L, Buhr F, Malik Ghulam M, Lerbs-Mache S (2011) Characterization of plastid psbT sense and antisense RNAs. Nucleic Acids Res 39: 5379-5387**

Pubmed: [Author and Title](#)

CrossRef: [Author and Title](#)

Google Scholar: [Author Only](#) [Title Only](#) [Author and Title](#)